

12359

P-50

12359

NASA CASE NO. NPO-18521-1-CU

PRINT FIG. 3a

**NOTICE**

The invention disclosed in this document resulted from research in aeronautical and space activities performed under programs of the National Aeronautics and Space Administration. The invention is owned by NASA and is, therefore, available for licensing in accordance with the NASA Patent Licensing Regulation (14 Code of Federal Regulations 1245.2).

To encourage commercial utilization of NASA-Owned inventions, it is NASA policy to grant licenses to commercial concerns. Although NASA encourages nonexclusive licensing to promote competition and achieve the widest possible utilization, NASA will consider the granting of a limited exclusive license, pursuant to the NASA Patent Licensing Regulations, when such a license will provide the necessary incentive to the licensee to achieve early practical application of the invention.

Address inquiries and all applications for license for this invention to NASA Patent Counsel, NASA Resident Office-JPL, Mail Code 180-801, 4800 Oak Grove Drive, Pasadena, CA 91109.

Approved NASA forms for application for nonexclusive or exclusive license are available from the above address.

Serial Number: 07/934,078

Filed Date: August 14, 1992

NRO-JPL

(NASA-CASE-NPO-18521-1-CU)  
REAL-TIME EDGE-ENHANCED OPTICAL  
CORRELATOR Patent Application  
(NASA) 50 0

N93-14404

October 7, 1992

Unclass

63/74 0123659

484/01

REAL-TIME EDGE-ENHANCED OPTICAL CORRELATOR

Serial No. 07/934,078  
 Filing Date 8-14-92  
 Contract No. NAS7-913  
 Contractor Caltech/JPL  
Pasadena CA  
 (City) JPL Case No. 18521-9110  
 (State)  
~~Nasa Case No. NPO-18521-91-CU~~

Inventors: Mazen M. Shihabi, Sami M Hinedi,  
 and Biren N. Shah

Contractor: Jet Propulsion Laboratory

August 14, 1992

AWARDS ABSTRACT

The invention relates to symbol lock detector for coherent digital communication systems after carrier and subcarrier, if any, synchronization has been achieved in a phase-locked loop employing nonoverlapping symbol intervals, where symbol data,  $d_k$ , takes on binary values with equal probability, and symbol interval  $T$  is known.

FIG. 1 is a generic functional block diagram, while FIGs. 2a and 2b are functional block diagrams of respective prior-art square-law symbol lock detector (SQOD) and prior-art absolute value symbol lock detector (AVOD), with integration of overlapping intervals in both cases, thus requiring separate integrators 21 and 22 in both cases. FIGs. 3a and 3b are functional block diagrams of a new nonoverlapping square-law symbol detector SQNOD and a new nonoverlapping absolute value detector AVNOD, respectively, that process nonoverlapping half symbol intervals ( $T/2$ ) so that a single integrator 30 may be used in each case with a multiplexer 32 for routing the inphase data through a half symbol interval delay element 33 to means for forming a difference  $X_k = I_k^2 - Q_k^2$  and accumulating a number,  $M$ , of  $X_k$  samples to form a statistic  $Y$  for threshold detection, all with functional blocks 26, 27 and 28 in series. A third new signal-power symbol lock detector (SPED) shown in FIG. 4 omits both the squaring operation 31 and the absolute value operation 31' of the embodiments of FIGs. 3a and 3b and instead utilizes a multiplexer 41 to connect the inphase data  $I_k$  through a delay element 42 to a multiplier 43 and to connect the quadrature data  $Q_k$  directly to the multiplier 43 to form a product  $X_k$  over many symbol intervals and thresholding an accumulation  $Y$  of  $M$  samples of the product  $X_k$  to form a symbol lock decision when the threshold  $\delta$  is exceeded. This provides greater simplicity in the implementation of a symbol lock detector with better performance when the threshold  $\delta$  is set in the presence of noise only (no signal) than even the prior-art symbol lock detectors which outperform the first two new symbol lock detectors of FIGs. 3a and 3b when the threshold is set in the presence of a signal. The first two new symbol lock detectors nevertheless provided sufficiently good performance for them to be considered for DSN communication receivers because of their advantage of requiring only one integrator. FIGs. 5a and 5b through FIG. 8 present graphs of analytical data which uphold these conclusions about performance.

The novelty of the invention resides in reaching a symbol lock decision by integrating nonoverlapping half symbol intervals so that only one time-shared integrator is required. An electronic multiplexing switch required in order to operate with just one integrator is very simple as compared to implementing a second integrator. A further improvement resides in forming the product (power) of the integrals of nonoverlapping half symbol data instead of first forming the squares or absolute values and then forming the sum of their differences.

JPL Case No. 18521  
NASA Case No. NPO-18521-1-CU  
F92143

Serial No.	07/934,078	
Filing Date	8-14-92	
<b>PATENT APPLICATION</b>		
Contract No.	N07-223	
Contractor	Calspan/PLB	
Pasadena	CA.	91109
(City)	(State)	(Zip)

**SYMBOL LOCK DETECTION IMPLEMENTED  
WITH NONOVERLAPPING INTEGRATION INTERVALS**

ORIGIN OF INVENTION

The invention described herein was made in the performance of work under a NASA contract, and is subject to the provisions of Public Law 96-517 (35 USC  
5 202) in which the contractor has elected not to retain title.

TECHNICAL FIELD

This invention relates to symbol lock detectors for coherent digital communication systems after  
10 carrier and subcarrier synchronization has been achieved in a phase lock loop, and more particularly to lock detectors which may be implemented with a single integrator for processing nonoverlapping symbol intervals of an incoming signal.

15 BACKGROUND ART

Deep space network (DSN) receivers currently under development use phase locked loops (PLLs) to track the carrier, subcarrier, and symbol phase. Like most coherent receivers, the DSN receivers rely on  
20 lock detectors to provide the symbol lock status of its PLLs. Since carrier, subcarrier, and symbol synchronization need to be achieved before any meaningful symbol detection can be initiated, symbol lock detectors play a vital role in the final decision of  
25 accepting or rejecting the detected symbols. In the past, symbol lock detectors have employed overlapping symbol intervals in their operations and therefore

require two integrators operating over staggered time intervals.

During operation, a loop is assumed to be locked when its lock indicator consistently has a positive status. The carrier and subcarrier lock detectors currently used in DSN receivers have already been analyzed. The present invention concerns the analysis of three new symbol lock detectors which simplify implementation for DSN receivers and two prior-art symbol lock detectors for comparison.

#### Statement of the Invention

In accordance with the present invention, an incoming signal that has undergone carrier and subcarrier (if any) synchronization is processed to determine whether or not symbol lock has also been achieved. The symbol data,  $d_k$ , takes on the binary values of a pulse  $p(t)$  of a known duration, such as in a nonreturn-to-zero (NRZ) or Manchester code, where the probability of the data having a +1 is equal to having a -1 (or 0) value, (i.e., the data transition probability equals one half). While the prior-art lock detectors employ two integrators for processing two overlapping symbol intervals, the lock detectors of the present invention require only one integrator for processing two nonoverlapping time intervals, e.g., integration of the last half of one ( $d_{k-1}/2$ ) and the first half ( $d_k/2$ ) of the next symbol interval, followed by integration of the second half ( $d_k/2$ ) of the next and the first half ( $d_{k+1}/2$ ) of the following symbol interval, or the first half of each symbol interval followed by the second half of each symbol interval. The receiver is assumed to have perfect

knowledge of the symbol interval  $T=kt$ , where  $k$  is the number of data bits, and  $t$  is the data bit interval.

The first integration output is processed and delayed a half symbol interval,  $T/2$ , for determining symbol lock by addition to or multiplication with the following integration output, where the processing of the first and second integration outputs is a squaring operation or an absolute value operation, and symbol lock is determined by addition of the processed second integration output to the processed first integration output delayed a half symbol interval and accumulating the sums. Symbol lock is then determined by repeatedly thresholding the accumulated sums every  $M$  symbol intervals. An alternative arrangement for determining symbol lock is by multiplying the second integration outputs by the first integration output delayed a half symbol interval to obtain a signal power estimation, and after accumulating signal power estimates over  $M$  symbol intervals, thresholding the accumulated estimates.

#### BRIEF DESCRIPTION OF THE DRAWINGS

FIG. 1 is a functional block diagram common to symbol lock detectors shown in FIGs. 2a through 4.

FIG. 2a is a functional block diagram of a prior-art square-law symbol lock detector with integration of overlapping intervals (SQOD).

FIG. 2b is a functional block diagram of a prior-art absolute-value symbol lock detector with integration of overlapping intervals (AVOD).

FIG. 3a is a functional block diagram of a square-law symbol lock detector with integration of

nonoverlapping intervals (SQNOD) in accordance with the present invention.

FIG. 3b is a functional block diagram of an absolute-value symbol lock detector with integration of nonoverlapping intervals (AVNOD) in accordance with the present invention.

FIG. 4 is a functional block diagram of a signal-power symbol lock estimator (SPED) with integration of nonoverlapping (first and second) halves of incoming signal symbols in accordance with the present invention.

FIG. 5a and 5b are graphs of the probability density function of the output  $Y$  for the SQOD of FIG. 2a when symbol lock is not present and the output  $Y$  has a high SNR=5dB and a low SNR=-5dB, respectively.

FIG. 6 is a graph of the probability of lock detection when  $\tau$  is an unknown constant over a decision interval for symbol lock detection of FIGs. 2a, 2b, 3a, 3b and 4.

FIG. 7 is a graph of the probability of lock detection versus SNR when  $\tau$  is uniformly distributed and changing from symbol to symbol for symbol lock detectors of FIGs. 2a, 2b, 3a, 3b and 4.

FIG. 8 is a graph of the probability of lock detection versus SNR when the false alarm rate is computed in the absence of a signal for symbol lock detectors of FIGs. 2a, 2b, 3a, 3b and 4.

#### DETAILED DESCRIPTION OF THE INVENTION

The symbol lock detectors considered are divided into two groups. The detectors in the first group are prior-art symbol lock detectors that process the overlapping outputs of two symbol data bit integra-

tors, whereas those in the second group, which depart from the prior art, use one integrator for two non-overlapping intervals of an incoming signal to determine whether or not symbol lock has been achieved.

5       The first group of symbol lock detectors employ either the squares of the two overlapping integrator outputs or the absolute value of the integrator outputs. The second group consists of three new lock detectors, two of which use the same mathematical  
10 operations of squaring or taking the absolute values of integration outputs of nonoverlapping half symbol intervals but only one integrator, while the third detector, which also uses only one integrator, does not include either squaring or absolute value operations,  
15 and instead functions as a signal power estimator by multiplying the two integration outputs of nonoverlapping half symbol intervals.

The five lock detectors are compared based on the lock-detection probability as a function of the symbol  
20 SNR for a given false-alarm probability and a fixed observation interval.

Although symbol lock detection has been addressed before [J.K. Holmes, *Coherent Spread Spectrum System*, New York: John Wiley and Sons, 1982 and K.T. Woo,  
25 *Shuttle Bit Synch Lock Detector Performance*, TRW IOC No. SCTE 50-76-184/KTW, TRW Corporation, El Segundo, California, April 5, 1976], the analyses have neglected the interdependence between symbol synchronizer bandwidth, and lock detector bandwidth. The  
30 symbol synchronizer bandwidth refers to the one-sided loop noise bandwidth  $B_L$  of the digital data-transition tracking loop [M. Simon, "An Analysis of the Steady-State Phase Noise Performance of a Digital Data-

Transition Tracking Loop," JPL *Space Programs Summary*, 37-55, Vol. 3, Jet Propulsion Laboratory, Pasadena, California, pp. 54-62, February 28, 1969] used in the receivers. The lock detector bandwidth is defined as  
5 the frequency at which the lock detector provides a status signal of being in or out-of-lock. For example, the lock detectors considered here indicate loop status once every  $M$  symbols. Consequently, the bandwidth of these detectors is  $1/MT$ , where  $T$  is the  
10 symbol interval.

The probability of false alarm,  $P_{fa}$ , is defined in two ways. In the classical sense, it is defined as the probability of declaring a signal (or target as in radar applications) to be present when it is not  
15 present. In deep space applications however, it is more appropriate to define  $P_{fa}$  as the probability of declaring a loop to be in-lock when it is out-of-lock. That is, declaring the timing error to be zero (in-lock) when the loop is slipping cycles and operating  
20 with a non-zero timing error (out-of-lock).

In discussion below, the false alarm rate is shown to be drastically different depending on the definition used. In addition when the loop is slipping cycles, the false alarm rate is shown to depend  
25 strongly on the ratio of the lock detector bandwidth to the symbol loop bandwidth. For example, when the loop is slipping and  $1/B_L \ll MT$  the lock detectors operate with acceptable false alarm rates because there are several uncorrelated samples of the timing  
30 error  $1/\tau$  within the  $MT$  second decision interval. On the other hand, when  $1/B_L \gg MT$  the false alarm rates are unacceptable because the timing error is constant over several decision intervals. Note that a good rule

of thumb is to assume that the loop provides uncorrelated phase estimates every  $1/B_L$  seconds. As a result, the symbol timing error at time  $t_i$  is uncorrelated with the symbol timing error at time  $t_j$  when  
 5  $|t_i - t_j| \geq 1/B_L$ . This article considers the special cases of  $1/B_L = MT$  and  $1/B_L = T$ . The first case is analyzed and simulated whereas, the second is simulated but not analyzed. When the threshold is adjusted in the presence of noise only, the performance can be  
 10 derived from the previous analysis by setting the signal amplitude to zero.

#### Generic Description of Lock Detectors

FIG. 1 is a block diagram showing the signal processing functions common to the *symbol lock detectors*  
 15 analyzed and discussed below, including both prior-art lock detectors of FIGs. 2a and 2b, and new lock detectors in accordance with the present invention as shown in FIGs. 3a, 3b, and 4. The received signal is assumed to have been mixed with perfect carrier and subcarrier  
 20 local reference signals so that the input to the lock detectors is a baseband signal of the form

$$r(t) = Ad(t) + n(t) \quad (1)$$

where  $A$  is the signal amplitude and  $A^2$  is the received data power with

$$d(t) = \sum_{k=-\infty}^{\infty} d_k p(t-kT) \quad (2)$$

and where  $n(t)$  is the additive white Gaussian noise process with a single-sided power spectral density (PSD)  $N_0$  (Watts/Hz). The data symbol  $d_k$  takes on the binary value +1 and -1 (or 0) with equal probability, and  $p(t)$  is the received data pulse shape of duration  $T$  seconds. For comparison purposes, only the NRZ pulse is considered in the analysis but the results can be extended to any pulse shape, such as Manchester encoded data. The receiver is assumed to have perfect knowledge of  $T$ , but not the symbol epoch, i.e., the receiver has estimated perfectly the symbol rate but not necessarily the start and end of the symbols.

The signal processing functions for the *symbol lock detector 10* in FIG. 1 depend on the processing of integration outputs in the detector. Its output  $X_k$  is at the symbol rate and typically many samples of  $X_k$  are averaged in an accumulator 12 to obtain the decision statistic  $Y$  compared in a block 14 with a threshold value  $\delta$ . If  $Y$  is greater than the threshold  $\delta$ , the loop is declared to be in-lock, otherwise it is declared to be out-of-lock.

The symbol timing error (parameter)  $\tau$  in FIG. 1 is the phase error between the symbol phase and the phase estimate provided by the symbol synchronizer. The in-lock case is analyzed by setting the timing error  $\tau$  to zero. In practice, the error is not identically zero, but it is a very small value. When there is a signal present, the out-of-lock model for  $\tau$  depends on the relation between  $B_L$  and  $1/(MT)$ . When  $B_L = 1/(MT)$ ,  $\tau$  is modeled as an unknown constant over a decision interval ( $MT$  seconds) but independent and uniformly distributed from one decision interval to the next.

Alternatively, when  $B_L = 1T$ , the timing error is modeled as constant over a symbol interval,  $T$ , but independent and uniformly distributed from symbol to symbol. In this case, if the decision time  $MT \gg T$  (as it usually is), each decision statistic encompasses the entire range of  $\tau$ . When there is no signal present, the model of  $\tau$  is irrelevant because the out-of-lock performance is independent of  $\tau$ .

The respective prior-art and new detectors considered and compared below are the square-law detector with overlapping (SQOD) and non-overlapping (SQNOD) integrators shown in FIGs. 2a and 3a, the absolute-value detectors with overlapping (AVOD) and non-overlapping (AVNOD) integrators shown in FIGs. 2b and 3b, and finally the new signal power estimator detector (SPED) shown in FIG. 4.

In the prior-art SQOD detector, FIG. 2a, the input signal  $r(t)$  is integrated over two symbol periods by two integrators 21 and 22: one in phase with the estimated symbol interval and the other staggered by half a symbol duration. The resulting inphase and quadrature samples  $I_k$  and  $Q_k$  are correlated due to the overlapping intervals. The quadrature samples  $I_k$  are squared in a processor 23 and delayed a half symbol period by a delay element 24 while the samples  $Q_k$  are squared in a processor 25. The delayed  $(I_k)^2$  and the undelayed  $(Q_k)^2$  samples are then combined in a summing circuit 26 to form an output  $X_k$  which are averaged in an accumulator 27 to obtain the decision statistic  $Y$  which is then compared with a predetermined threshold  $\delta$  in a detector 28 to reach a lock decision. The prior-art AVOD detector, FIG. 2b merely replaces the squaring operations in FIG. 2a with absolute value

operations in blocks 23' and 25'. Hence, the  $I$  and  $Q$  samples of the prior-art AVOD detector are also correlated.

The new SQNOD detector, FIG. 3a, processes the  
5 integration outputs of nonoverlapping half symbol intervals from a single integrator 30. A single squaring operation in block 31 produces the square of the integration outputs from both halves of a symbol interval, and a multiplexer separates the first and  
10 second half symbol interval integration outputs sending the first half through a delay element of half a symbol interval and the second half directly to a summing circuit 34. Its output  $X_k$  is then averaged in an accumulator 35 and its output, and the decision  
15 statistic  $Y$  is compared with a threshold  $\delta$  in a detector 36. As before, replacing the squaring operations in FIG. 3a with absolute value operations in block 31' yields its counterpart the AVNOD detector shown in FIG. 3b. The integrator outputs in these  
20 cases are uncorrelated because the integrated intervals are nonoverlapping.

The SPED detector shown in FIG. 4, which also uses a single integrator 40, was considered for symbol lock detection because it already existed as part of  
25 a split symbol moment SNR estimator [K.T. Woo, *supra*] in DSN receivers used for SNR estimation. The inphase ( $I_k$ ) and quadrature ( $Q_k$ ) integration outputs of the SPED are obtained by integrating the received signal over the respective first and second halves of a  
30 symbol interval and separating them by a multiplexer 41. Since the noise in the first and second half are independent, delaying the inphase integration output,  $I_k$ , in a delay element 42 and then forming the product

of  $I_k$  and  $Q_k$  in a multiplexer 43 and averaging over number,  $M$ , of symbol intervals in an accumulator 44, provides as a decision statistic  $Y$  an estimate proportional to signal power which is then compared to the value  $\delta$  in a threshold detector 45 to provide a lock decision.

### Performance Analysis

In-lock performance is measured in terms of the probability of declaring a phase-locked loop (PLL) as being symbol locked when there is no timing error, i.e., the probability that the decision statistic  $Y$  is greater than the threshold value  $\delta$  when  $\tau = 0$ . Note that  $\tau = 0$ , or no phase tracking error, is equivalent to setting the symbol synchronizer loop SNR to infinity. The degradation in detection probability due to timing jitter (non-infinite loop SNR) is minimal and has been addressed in the case of carrier lock detectors [A. Mileant and S. Hinedi, "Costas Loop Lock Detection in the Advanced Receiver," TDA Progress Report 42-99, Vol. July-September 1989, Jet Propulsion Laboratory, Pasadena, California pp. 72-89, November 15, 1989]. The out-of-lock performance is measured by the probability of false alarm, i.e., the probability of declaring the loop as locked when it is not locked. The out-of-lock performance in the presence of a signal is analyzed for the case  $B_L = 1/(MT)$ . Note that, in that case, the timing error  $\tau$  is independent from one symbol to another and the decision is performed after averaging a number,  $M$ , of symbols. On the other hand when  $B_L = 1/(MT)$ ,  $\tau$  is an unknown constant during a decision interval and independent from one decision to the next. Setting  $M = 1$  in the

latter case would imply a decision every symbol, which is fundamentally different from the case  $B_L = 1/T$  decision using  $M$  symbols. Hence, the performance when  $B_L = 1/T$  cannot be derived from the case of  $B_L = 1/(MT)$ , simply by setting  $M = 1$ . The out-of-lock performance when there is no signal present is also analyzed.

In this discussion, only the final equations are shown. Derivations of these equations are set forth in the various appendices A through F for all five symbol lock detectors SQOD, SQNOD, AVOD, AVNOD and SPED which, by this reference, are hereby made a part hereof. In all cases, the decision statistic can be expressed as the average of samples  $X_k$  over  $M$  symbol intervals given by the equation

$$Y = \frac{1}{M} \sum_{k=1}^M X_k \quad (3)$$

Note that the random variable  $X_k$  is peculiar to each detector. When the timing offset  $\tau = 0$ , the adjacent samples  $X_k$  and  $X_{k+1}$  are correlated in the two prior-art detectors (SQOD and SQNOD), whereas for the three new detectors (AVOD, AVNOD and SPED) they are uncorrelated. In all cases, the random variable  $X_k$  is not Gaussian due the nonlinear operations on  $I_k$  and  $Q_k$ . For large  $M$ , the random variable  $Y$  is modeled as Gaussian due to the Central Limit Theorem (CLT). The CLT theorem applies to the sum of correlated random variables when none of the variables being summed or multiplied dominates over the others [D. Fraser, *Non-Parametric Methods in Statistics*, New York: John Wiley and Sons, 1957]. This model for  $Y$  is justified

by simulation results. The probability of lock detection is the probability that the Gaussian random variable  $Y$  surpasses the threshold  $\delta$ . Hence, it is given by

$$P_D = \int_{\delta}^{\infty} \frac{1}{\sqrt{2\pi\sigma_Y^2}} \exp\left[-\frac{(y-\mu_Y)^2}{2\sigma_Y^2}\right] dy \quad (4)$$

5 where  $\mu_Y$  and  $\sigma_Y^2$  are the mean and variance of  $Y$  when  $\tau$  is exactly zero. Using the definition of the error function

$$\operatorname{erf}(x) \triangleq \frac{2}{\sqrt{\pi}} \int_0^x \exp(-t^2) dt \quad (5)$$

one has

$$P_D = \frac{1}{2} - \frac{1}{2} \operatorname{erf}\left(\frac{\delta - \mu_Y}{\sqrt{2}\sigma_Y}\right) \quad (6)$$

or

$$P_D = \frac{1}{2} - \frac{1}{2} \operatorname{erf}\left(\frac{\delta}{\sqrt{2}\sigma_Y} \sqrt{\frac{\operatorname{SNR}_D}{2}}\right) \quad (7)$$

10 where  $\operatorname{SNR}_D$  denotes the detector SNR defined by

$$\operatorname{SNR}_D \triangleq \left(\frac{\mu_Y}{\sigma_Y}\right)^2 \quad (8)$$

The threshold  $\delta$  is chosen to maintain a fixed probability of false alarm. The probability of false alarm is the probability that the out-of-lock decision statistics do not surpass the threshold. Hence, it is  
 5 given by

$$P_{fa} = \int_{-\infty}^{\delta} f_o(y) dy \quad (9)$$

where  $f_o(y)$  is the out-of-lock density of  $Y$ . The threshold  $\delta$  is computed by solving Eq. (9) for a fixed  $P_{fa}$ . When there is a signal present and  $B_L = 1/(MT)$ , the statistic  $Y$  is no longer Gaussian and  $f_o(y)$  must  
 10 be obtained numerically or by simulation as shown below. When there is no signal present, the CLT can be invoked and the out-of-lock decision statistic can be modeled as Gaussian. This model is verified by simulations below. In this case, Eq. (9) can be  
 15 written as

$$P_{fa} = \frac{1}{2} - \frac{1}{2} \operatorname{erf} \left( \frac{\delta - \mu_{Y_0}}{\sqrt{2}\sigma_{Y_0}} \right) \quad (10)$$

where  $\mu_{Y_0}$  and  $\sigma_{Y_0}$  the out-of-lock mean and variance of the decision statistic  $Y$ . The threshold  $\delta$  is given by

$$\delta = \sqrt{2}\sigma_{Y_0}\gamma + \mu_{Y_0} \quad (11)$$

where  $\gamma = \operatorname{erf}^{-1}(1 - 2P_{fa})$ . Substituting Eq. (11) into Eq. (6) relates the probability of detection to the no  
 20 signal (classical) false alarm rate, namely,

$$P_D = \frac{1}{2} - \frac{1}{2} \operatorname{erf} \left( \frac{\sqrt{2}\sigma_{r_0}\gamma + \mu_{r_0} - \mu_r}{\sqrt{2}\sigma_r} \right) \quad (12)$$

The next five subsections derive the in-lock and out-of-lock mean and variance for all five detectors SQOD, SQNOD, AVOD, AVNOD and SPED for comparison.

5 (1). Square-Law Lock Detector with Overlapping Intervals (SQOD)

The SQOD detector is shown in FIG. 2a. For the input given by Eq. (1), the inphase integrator output is given by

$$\begin{aligned} I_k &= \int_{kT+\tau}^{(k+1)T+\tau} r(t) dt \\ &= d_k A (T-\tau) + d_{k+1} A \tau + N_1(k) + N_2(k) \end{aligned} \quad (13)$$

and the quadrature integrator output is given by

$$\begin{aligned} Q_k &= \int_{(k+\frac{1}{2})T+\tau}^{(k+\frac{3}{2})T+\tau} r(t) dt \\ &= \begin{cases} d_k A \left( \frac{T}{2} - \tau \right) + d_{k+1} A \left( \frac{T}{2} + \tau \right) \\ \quad + N_2(k) + N_1(k+1) & 0 \leq \tau < \frac{T}{2} \\ d_{k+1} A \left( \frac{3T}{2} - \tau \right) + d_{k+2} A \left( \tau - \frac{T}{2} \right) \\ \quad + N_2(k) + N_1(k+1) & \frac{T}{2} \leq \tau < T \end{cases} \end{aligned} \quad (14)$$

where  $\tau$  is limited to the interval  $[0, T]$ , and where

$$N_1(k) = \int_{kT+\tau}^{(k+\frac{1}{2})T+\tau} n(t) dt \quad (15)$$

and

$$N_2(k) = \int_{(k+\frac{1}{2})T+\tau}^{(k+1)T+\tau} n(t) dt \quad (16)$$

Since  $n(t)$  is a white Gaussian process with one-sided  
 5 PSD  $N_o$ , the  $N_i$ 's are independent Gaussian random variables with mean zero and variance  $\sigma_n^2 = (N_o T) / 4$ . The samples  $X_k = I_k^2 - Q_k^2$  and summing  $M$  of them yields  $Y$ . From Appendix A, the in-lock mean and variance of  $Y$  are given by

$$\mu_Y = \frac{\eta_s N_o T}{2} \quad (17)$$

10 and

$$\sigma_Y^2 = \left( \frac{N_o T}{M} \right)^2 \left[ M \left( \frac{\eta_s^2}{4} + 2\eta_s + \frac{3}{4} \right) \right. \\ \left. + 2(M-1) \left( -\frac{\eta_s}{2} - \frac{1}{8} \right) \right] \quad (18)$$

The out-of-lock mean and variance when there is a signal present and  $\tau$  is an unknown constant over a decision interval ( $B_L = 1/(MT)$ ) are given by

$$\mu_{Y_o} = 0.0 \quad (19)$$

$$\sigma_{Y_o}^2 = \left(\frac{N_o T}{M}\right)^2 \left[ M \left( \frac{31\eta_s^2}{120} + \frac{41\eta_s}{24} + \frac{3}{4} \right) + 2(M-1) \right. \\ \left. X \left( \frac{23\eta_s^2}{320} - \frac{23\eta_s}{48} - \frac{1}{8} \right) + (M-1)(M-2) \frac{\eta_s^2}{12} \right] \quad (20)$$

where  $\eta_s$  denotes symbol signal-to-noise ratio and is defined as

$$\eta_s \triangleq \frac{A^2 T}{N_o} \quad (21)$$

Setting  $A = 0$  in Eq. (20) and substituting the result in Eqs. (19) and (20) yields the out-of-lock mean and variance in the no signal case. Hence, the no signal mean is zero but the no signal variance is given by

$$\sigma_{Y_o}^2(\eta_s=0) = \left(\frac{N_o T}{M}\right)^2 \left[ M \frac{3}{4} - 2(M-1) \frac{1}{8} \right] \quad (22)$$

## (2). Absolute-Value Lock Detector with Overlapping Intervals (AVOD)

For the AVOD detector shown in FIG. 2b, absolute values are used instead of squares. The expressions

for  $I_k$  and  $Q_k$  given by Eqs. (13) and (14) are still valid but now  $X_k = |I_k| - |Q_k|$ . From Appendix B, the in-lock mean and variance are given by

$$\mu_Y = \left( \sqrt{\frac{N_o T}{4}} \right) \left[ \frac{\exp(-\eta_s) - 1}{\sqrt{\pi}} + \sqrt{\eta_s} \operatorname{erf}(\sqrt{\eta_s}) \right] \quad (23)$$

and

$$\sigma_Y^2 = \frac{1}{M^2} [M \operatorname{Var}(X_k) + M(M-1) \operatorname{Cov}(X_k, X_{k+1})] \quad (24)$$

5 where

$$\begin{aligned} \operatorname{Var}(X_k) = (N_o T) & \left\{ \frac{3\eta_s + 1 - \eta_s [F_1(\eta_s) + F_2(\eta_s)]}{2} \right. \\ & - \frac{1}{4\pi} [\exp(-2\eta_s) - 2\exp(-\eta_s) + 1] - \frac{\eta_s}{4} \operatorname{erf}^2(\sqrt{\eta_s}) \\ & \left. - \frac{1}{2} \sqrt{\frac{\eta_s}{\pi}} \operatorname{erf}(\sqrt{\eta_s}) [\exp(-\eta_s) - 1] \right\} \quad (25) \end{aligned}$$

and

$$\operatorname{Cov}(X_k, X_{k+1}) = (N_o T) \left\{ \frac{\exp(-2\eta_s) + \exp(-\eta_s)}{2\pi} \right\}$$

$$\begin{aligned}
& + \frac{\eta_s}{2} \operatorname{erf}^2(\sqrt{\eta_s}) + \left[ \exp(-\eta_s) + \frac{1}{2} \right] \operatorname{erf}(\sqrt{\eta_s}) \\
& \left. x \sqrt{\frac{\eta_s}{\pi}} - \frac{\eta_s}{2} [F_1(\eta_s) + F_2(\eta_s)] \right\} \quad (26)
\end{aligned}$$

The out-of-lock mean and variance when there is a signal and  $\tau_0$  is constant over  $M$  symbols are given by

$$\mu_{y_0} = 0.0 \quad (27)$$

and

$$\begin{aligned}
\sigma_{y_0}^2 = \frac{1}{M^2} [M \operatorname{Var}_o(X_k) + 2(M-1) \operatorname{Cov}_o(X_k, X_{k+1}) \\
+ (M-1)(M-2) \operatorname{Cov}_o(X_k, X_{k+2})] \quad (28)
\end{aligned}$$

5 where

$$\begin{aligned}
\operatorname{Var}_o(X_k) = (N_o T) \left\{ \frac{4\eta_s}{3} + 1 - \eta_s \left[ \frac{3}{4} F_1(\eta_s) + G_1(\eta_s) \right. \right. \\
\left. \left. + \frac{H_1(\eta_s) + H_2(\eta_s) + H_3(\eta_s)}{2} \right] \right\} \quad (29)
\end{aligned}$$

$$\begin{aligned}
\text{Cov}_o(X_k, X_{k+1}) = & (N_0T) \left\{ \frac{\exp(-2\eta_s)}{2\pi} + \left( \frac{\eta_s}{2} + \frac{1}{8} \right) \right. \\
& \times \text{erf}^2(\sqrt{\eta_s}) + \exp(-\eta_s) \text{erf}(\sqrt{\eta_s}) \left( \sqrt{\frac{\eta_s}{\pi}} + \frac{1}{8\sqrt{\pi\eta_s}} \right) \\
& + \frac{\eta_s}{4} [F_3(\eta_s) + G_3(\eta_s) + H_4(\eta_s) - G_4(\eta_s) - H_5(\eta_s) \\
& \left. - \frac{3}{2} F_1(\eta_s) - G_1(\eta_s) - 2G_2(\eta_s) - 2H_2(\eta_s)] \right\} \quad (30)
\end{aligned}$$

$$\begin{aligned}
\text{Cov}_o(X_k, X_{k+j}) = & \left( \frac{N_0T\eta_s}{4} \right) [F_3(\eta_s) + G_3(\eta_s) + H_4(\eta_s) \\
& - 2G_4(\eta_s) - 2H_5(\eta_s)] \quad \text{for } j \geq 2 \quad (31)
\end{aligned}$$

The functions  $F_i$ ,  $G_i$  and  $H_i$  in Eqs. (28) through (31) are defined in Appendix B and plotted in Fig. B.1 versus  $\eta_s$ . Setting  $\eta_s = 0$  in Eqs. (28) through (31) yields the out-of-lock statistics in the no signal case. The no signal mean is zero but the variance is given by

$$\sigma_{Y_o}^2(\eta_s=0) = \left( \frac{N_0T}{M^2} \right) \left[ M+2(M-1) \left( \frac{1}{2\pi} \right) \right] \quad (32)$$

(3). Square-Law Lock Detector with Nonoverlapping Intervals (SQNOD)

The SQNOD detector is shown in Fig. 2b. For the input of Eq. (1), The inphase and quadrature integrator outputs are given by

$$\begin{aligned}
 I_k &= \int_{(k+\frac{1}{4})T+\tau}^{(k+\frac{3}{4})T+\tau} r(t) dt \\
 &= \begin{cases} d_k \frac{AT}{2} + N_1(k) & 0 \leq \tau < \frac{T}{4} \\ d_k A \left( \frac{3T}{4} - \tau \right) \\ \quad + d_{k+1} A \left( \tau - \frac{T}{4} \right) + N_1(k) & \frac{T}{4} \leq \tau < \frac{T}{2} \end{cases} \quad (33)
 \end{aligned}$$

and

$$\begin{aligned}
 Q_k &= \int_{(k-\frac{1}{4})T+\tau}^{(k+\frac{1}{4})T+\tau} r(t) dt \\
 &= \begin{cases} d_{k-1} A \left( \frac{T}{4} - \tau \right) \\ \quad + d_k A \left( \frac{T}{4} + \tau \right) + N_2(k) & 0 \leq \tau < \frac{T}{4} \\ d_k \frac{AT}{2} + N_2(k) & \frac{T}{4} \leq \tau < \frac{T}{2} \end{cases} \quad (34)
 \end{aligned}$$

The noises  $N_1(k)$  and  $N_2(k)$  are given by Eqs. (15) and (16) after changing the integration limits to those in Eqs. (33) and (34). As a result, they are independent Gaussian random variables with zero mean and variance

$\sigma_n^2 = (N_o T) / 4$ . The sample  $X_k$  is the difference of the squares (i.e.,  $X_k = I_k^2 - Q_k^2$ ). From Appendix D, the in-lock mean and variance of  $Y$  are given by

$$\mu_Y = \frac{\eta_s N_o T}{8} \quad (35)$$

and

$$\sigma_Y^2 = \left( \frac{N_o^2 T^2}{M} \right) \left( \frac{\eta_s^2 + 24\eta_s + 16}{64} \right) \quad (36)$$

- 5 For the case of false lock with signal present and  $\tau$  an unknown constant over  $M$  symbols, one obtains

$$\mu_{Y_o} = 0.0 \quad (37)$$

and

$$\sigma_{Y_o}^2 = \left( \frac{N_o^2 T^2}{M^2} \right)$$

$$X \left[ M \left( \frac{\eta_s^2 + 25\eta_s + 15}{60} \right) + M(M-1) \frac{\eta_s^2}{120} \right] \quad (38)$$

- When there is no signal present the out-of-lock mean is zero and the variance is given by setting  $\eta_s = 0$  in  
 10 Eq. (38). Consequently, the no signal out-of-lock variance is

$$\sigma_{y_o}^2(\eta_s=0) = \left(\frac{N_o^2 T^2}{M}\right) \left(\frac{15}{60}\right) \quad (39)$$

(4). Absolute-Value Lock Detector with Nonoverlapping Intervals (AVNOD)

This detector shown in FIG. 3b is the same as the SQNOD detector shown in FIG. 3a with the squaring operations replaced by absolute value operations. Hence, Eqs. (32) and (33) for  $I_k$  and  $Q_k$  are valid but now  $X_k = |I_k| - |Q_k|$ . From Appendix E, the in-lock statistics for  $Y$  are given by

$$\mu_y = \sqrt{\frac{N_o T}{4}} \left[ \frac{\exp\left(-\frac{\eta_s}{2}\right) - 1}{\sqrt{2\pi}} + \frac{\sqrt{\eta_s}}{2} \operatorname{erf}\left(\sqrt{\frac{\eta_s}{2}}\right) \right] \quad (40)$$

and

$$\begin{aligned} \sigma_y^2 = & \left(\frac{N_o T}{M}\right) \left\{ \frac{3\eta_s}{8} + \frac{1}{2} - \frac{1}{8\pi} \left[ 1 + 5 \exp(-\eta_s) \right. \right. \\ & \left. \left. + 2 \exp\left(-\frac{\eta_s}{2}\right) \right] - \sqrt{\frac{\eta_s}{32\pi}} \operatorname{erf}\left(\sqrt{\frac{\eta_s}{2}}\right) \right. \\ & \left. \times \left[ 5 \exp\left(-\frac{\eta_s}{2}\right) + 1 \right] - \frac{5\eta_s}{16} \operatorname{erf}^2\left(\sqrt{\frac{\eta_s}{2}}\right) \right\} \quad (41) \end{aligned}$$

10 The out-of-lock mean and variance when there is a signal present and  $\tau$  an unknown constant over  $MT$  seconds is given by

$$\mu_{Y_o} = 0.0 \quad (42)$$

and

$$\sigma_{Y_o}^2 = \frac{1}{M^2} [M \text{Var}_o(X_k) + M(M-1) \text{Cov}_o(X_k, X_{k+1})] \quad (43)$$

$$\begin{aligned} \text{Var}_o(X_k) = (N_0 T) & \left[ \frac{5\eta_s}{12} + \frac{1}{2} - \frac{3}{4\pi} \exp(-\eta_s) \right. \\ & - \text{erf}^2 \left( \sqrt{\frac{\eta_s}{2}} \right) \left( \frac{1+3\eta_s}{8} \right) - \exp \left( -\frac{\eta_s}{2} \right) \\ & \left. \times \text{erf} \left( \sqrt{\frac{\eta_s}{2}} \right) \left( \frac{3}{2} \sqrt{\frac{\eta_s}{2\pi}} + \frac{1}{\sqrt{32\pi\eta_s}} \right) \right] \quad (44) \end{aligned}$$

$$\begin{aligned} \text{Cov}_o(X_k, X_{k+1}) = (N_0 T) & \left\{ -\frac{1}{16} \text{erf}^2 \left( \sqrt{\frac{\eta_s}{2}} \right) - \exp \left( -\frac{\eta_s}{2} \right) \right. \\ & \left. \times \text{erf} \left( \sqrt{\frac{\eta_s}{2}} \right) \left( \frac{1}{8\sqrt{2\pi\eta_s}} \right) + \frac{\eta_s}{2} Z(\eta_s) \right\} \quad (45) \end{aligned}$$

where the function  $Z$  is defined in Appendix E and plotted in Fig. B.2.

For the out-of-lock case with no signal, the mean is zero and the variance is obtained by setting  $\eta_s = 0$  in Eqs. (43) through (45). Hence, the out-of-lock variance is given by

$$\sigma_{Y_o}^2(\eta_s=0) = \frac{N_o T}{M} \left( \frac{1}{2} - \frac{3}{4\pi} \right) \quad (46)$$

**(5). Signal-Power Estimator Lock Detector (SPED)**

In the detector shown in FIG. 4, denote the integrations over the first half of the assumed symbol interval as  $I_k$  and the second half as  $Q_k$ . Then, the  $I_k$  and  $Q_k$  samples are given by

$$I_k = d_k \frac{AT}{2} + N_1(k) \quad (47)$$

and

$$Q_k = d_k A \left( \frac{T}{2} - \tau \right) + d_{k+1} A \tau + N_2(k) \quad (48)$$

and  $X_k = I_k Q_k$ . From Appendix F, the in-lock mean and variance of  $Y$  are

$$\mu_Y = \frac{\eta_s N_o T}{4} \quad (49)$$

and

$$\sigma_Y^2 = \left( \frac{N_o^2 T^2}{M} \right) \left( \frac{2\eta_s + 1}{16} \right) \quad (50)$$

The out-of-lock case with signal present has mean and variance when  $\tau$  is constant over  $M$  symbols is given by

$$\mu_{y_o} = \frac{\eta_s N_o T}{8} \quad (51)$$

and

$$\sigma_{y_o}^2 = \frac{N_o^2 T^2}{M^2} \left[ M \left( \frac{5\eta_s^2 + 20\eta_s + 12}{192} \right) + M(M-1) \frac{\eta_s^2}{192} \right] \quad (52)$$

As before, the out-of-lock variance in the no signal  
5 case is given by

$$\sigma_{y_o}^2(\eta_s=0) = \left( \frac{N_o^2 T^2}{M} \right) \left( \frac{12}{192} \right) \quad (53)$$

#### Discussion and Simulation Results

Digital simulation was used to verify the foregoing analysis. In the out-of-lock state for a long-time constant  $B_L = 1/(MT)$ , the symbol timing error  $\tau$   
10 is modeled as constant over a decision interval ( $MT$  seconds) but independent and uniformly distributed over the collection of all decision intervals. The timing error in the in-lock state is modeled as being zero. Although the special case of  $\tau$  constant over  $M$   
15 symbols was analyzed for performance comparison purposes, it is not advisable to operate a practical system under these conditions due to unacceptable false alarm rates. This case has higher than usual

false alarm rates because the decision statistic for small values of  $\tau$  is not significantly different from the statistic for  $\tau = 0$ . As a result, the out-of-lock states corresponding to small values of  $\tau$  are frequently declared to be in-lock because they are mistaken for the case when  $\tau = 0$ . This problem can be ameliorated by lengthening the observation time relative to the time constant of  $\tau$  (i.e., shortening the time constant of  $\tau$ ). In practice, it is recommended that the observation time be at least ten times longer than the time constant of  $\tau$ . As noted above, the out-of-lock density function for  $Y$  in this case is not Gaussian. Consider the decision statistic  $Y$  when the loop is out of lock and  $\tau$  is constant over  $M$  symbols. In general, it can be written as

$$X_k = s_k(\tau) + n_k + s_k(\tau)n_k \quad (54)$$

where, in all five detectors, the signal term  $s_k$  is random and uniformly distributed because  $\tau$  is a uniformly distributed random variable. The density of the noise  $n_k$  depends on the detector being implemented. Summing  $M$  samples of  $X_k$ , where  $X_k$  is at the symbol rate in all cases, yields the decision variable  $Y$ . Since  $\tau$  is constant over the sum, at high SNR (i.e., for strong signal levels) the density function of  $Y$  approaches a uniform distribution as shown in FIG. 5a. However, at low SNR the noise term dominates and the density of  $Y$  is Gaussian due to the central limit theorem as shown in FIG. 5b. The density in FIGS. 5a and 5b was obtained via numerical integration as well as simulation. Both methods are seen to agree very well. The numerical method computed the density

function of  $Y$ ,  $f(y)$ , by averaging over  $\tau$  the conditional pdf  $f(y/\tau)$ . The latter is Gaussian with mean and variance both a function of  $\tau$ . The simulation method computed the histogram of  $Y$  and then set  
5  $f(y)=[P(y-\Delta \leq Y \leq y+\Delta)]/\Delta$ , where  $\Delta$  is the size of a histogram bin. The histograms were generated using 1,00,000 million symbols which corresponds to 10,000 decisions ( $Y$ 's), since there are 100 symbols/decision.

FIG. 6 compares the probability of detection  
10 performance of all five detectors for  $M=100$  and  $P_{fa} = 0.25$ . Note that the overlapping detectors SQOD and AVOD, which are identical except for the squaring and absolute value operations, have nearly identical performance. As expected, the AVOD is slightly better  
15 at high SNR, whereas the SQOD is slightly better at low SNR. The non-overlapping detectors SQNOD and AVNOD also have nearly equal performance. Once again, the absolute value operation yield better results at higher SNRs. The signal level estimator (SPED) is  
20 better than the non-overlapping detectors but worse than the overlapping detectors. The probability of detection results in FIG. 6 change when  $P_{fa}$  or  $M$  change. For example, increasing the observation interval increases the detection probability because  
25 it increases the detector  $SNR = (\mu_Y^2/\sigma_Y^2)$ . Accepting a higher false alarm rate increases the probability of detection because it lower the threshold  $\delta$ . In generating these curves, 50,000 symbols were simulated for each value of SNR. Since there are 100 sym-  
30 bols/decision, the detection probability for a given SNR is based on 500 decisions.

In the out-of-lock state for a short-time constant ( $B_L = 1/T$ ), the symbol timing error  $\tau$  is modeled as uniformly distributed random variable that changes independently from symbol-to-symbol. For this case, the probabilities of detection for all five detectors are computed by simulation for  $M = 100$ ,  $P_{fa} = 10^{-2}$  and the threshold  $\delta$  is set according to Eq. (11). The false alarm rate was verified by simulation. The results are plotted in FIG. 7 versus symbol energy-to-noise ratio  $\eta_s$ . In these computer simulations, the detection probability for a given SNR is based on 40,000 decisions.

The results show that, the AVOD performs slightly better than SQOD at high SNR, whereas they seem to perform identically at low SNR. The nonoverlapping detectors SQNOD and AVNOD also have nearly equal performance at low SNR, but AVNOD performs about 1 dB better for values of symbol SNR higher than -4 dB. As far as the SPED, it performs about 2 dB worse than the overlapping detectors and 3 dB better than the other two nonoverlapping detectors. Also by simulation, the false-alarm rate that was used in setting the threshold was verified.

In the situation of no signal, i.e., when there is no signal present as distinguished from the case when there is a signal and  $\tau = 0$ , the out-of-lock statistic is Gaussian with zero mean and the in-lock statistic is Gaussian with non-zero mean. Probability of detection results are compared in FIG. 8. Interestingly, the performance of the overlapping and nonoverlapping detectors are grouped together, but the signal level detector (SPED) now has the best perfor-

mance. The interdependence between  $P_d$ ,  $P_{fa}$  and  $M$  is the same as in the other two cases.

### Conclusion

The performance of two prior-art symbol lock detectors shown in FIGs. 2a and 2b have been compared with three new ones shown in FIGs. 3a, 3b and 4. They are the square-law detector with overlapping (SQOD) compared with nonoverlapping (SQNOD) integrators and others, the absolute value detectors with overlapping (AVOD) compared with nonoverlapping (AVNOD) integrators and others, and the signal power estimator detector (SPED) compared with all others. The analysis considered various scenarios when the observation interval is much larger or equal to the symbol synchronizer loop bandwidth, which has not been considered in previous analyses. Also, the case of threshold setting in the absence of signal was considered. The analysis has shown that the square-law detector with overlapping integrators (SQOD) outperforms all others when the threshold is set in the presence of a signal, independent of the relationship between loop bandwidth and observation period. The square-law detector and absolute-value detector with overlapping integrators outperformed corresponding detectors with nonoverlapping integrators, but implementation of the SQOD and AVOD require two separate integrators since both integrators must operate at the same time due to overlapping, whereas the SQNOD and AVNOD symbol lock detectors may use a single interval since the separate integration operations required do not overlap in time. On the other hand, the signal-power estimator detector (SPED) outperforms all others when the

threshold  $\delta$  is set in the presence of noise only, and it requires only a single integrator for implementation.

SYMBOL LOCK DETECTION IMPLEMENTED  
WITH NONOVERLAPPING INTEGRATION INTERVALSABSTRACT OF THE DISCLOSURE

The performance of five symbol lock detectors are  
5 compared. They are the square-law detector with  
overlapping (SQOD) and non-overlapping (SQNOD) inte-  
grators, the absolute value detectors with overlapping  
and non-overlapping (AVNOD) integrators and the signal  
power estimator detector (SPED). The analysis consid-  
10 ers various scenarios when the observation interval is  
much larger or equal to the symbol synchronizer loop  
bandwidth, which has not been considered in previous  
analyses. Also, the case of threshold setting in the  
absence of signal is considered. It is shown that the  
15 SQOD outperforms all others when the threshold is set  
in the presence of signal, independent of the rela-  
tionship between loop bandwidth and observation  
period. On the other hand, the SPED outperforms all  
others when the threshold is set in the presence of  
20 noise only.

## Appendix A

### Derivation of the Mean and Variance of the SQOD

The inphase and quadrature integrator outputs are given by Eqs. (13) and (14), respectively. The output of the lock detector  $X_k = I_k^2 - Q_k^2$ . Consequently,

$$\mu_k = \mathcal{E}\{I_k^2\} - \mathcal{E}\{Q_k^2\} \quad (\text{A-1})$$

where  $\mu_k = \mathcal{E}\{X_k\}$ .

$$\begin{aligned} \text{Var}(X_k) &= \mathcal{E}\{(I_k^2 - Q_k^2)^2\} - \mathcal{E}^2\{I_k^2 - Q_k^2\} \\ &= \mathcal{E}\{I_k^4 + Q_k^4 - 2I_k^2 Q_k^2\} - \mu_k^2 \end{aligned} \quad (\text{A-2})$$

The covariance of  $X_k$  with  $X_{k+j}$  is

$$\text{Cov}(X_k, X_{k+j}) = \mathcal{E}\{I_k^2 I_{k+j}^2\} + \mathcal{E}\{Q_k^2 Q_{k+j}^2\} - \mathcal{E}\{I_k^2 Q_{k+j}^2\} - \mathcal{E}\{I_{k+j}^2 Q_k^2\} - \mu_k \mu_{k+j} \quad (\text{A-3})$$

When the loop is in lock, Eqs. (A-1) through (A-3) are evaluated with  $\tau$  set to zero in Eqs. (A-10) through (A-18). Hence, the in-lock moments of  $X_k$  are given by

$$\text{Var}(X_k) = \frac{A^4 T^4}{4} + 8A^2 T^2 \sigma_n^2 + 12\sigma_n^4 \quad (\text{A-4})$$

and

$$\text{Cov}(X_k, X_{k+1}) = -2A^2 T^2 \sigma_n^2 - 2\sigma_n^4 \quad (\text{A-5})$$

and for  $j \geq 2$ , this can be shown to be

$$\text{Cov}(X_k, X_{k+j}) = 0 \quad (\text{A-6})$$

When the loop is out-of-lock,  $\tau$  is modelled as a uniform random variable. Using this model for  $\tau$  in Eqs. (A-10) through (A-18) and substituting the results into Eqs. (A-1) through (A-3) give the out-of-lock moments of  $X_k$ . Namely, (where the additional subscript  $o$  denotes out-of-lock),

$$\text{Var}_o(I_k^2 - Q_k^2) = \frac{31A^4 T^4}{120} + \frac{41}{6} A^2 T^2 \sigma_n^2 + 12\sigma_n^4 \quad (\text{A-7})$$

$$\text{Cov}_o(X_k, X_{k+1}) = \frac{23A^4 T^4}{320} - \frac{23}{12} A^2 T^2 \sigma_n^2 - 2\sigma_n^4 \quad (\text{A-8})$$

and for  $j \geq 2$ , this can be shown to be

$$\text{Cov}_o(X_k, X_{k+j}) = \frac{A^4 T^4}{12} \quad (\text{A-9})$$

The following equations were used to compute the variance of  $X_k$  and covariance of  $X_k$  with  $X_{k+1}$ :

$$\mathcal{E}\{I_k^2\} = A^2(T^2 - 2T\mathcal{E}\{\tau\} + 2\mathcal{E}\{\tau^2\}) + 2\sigma_n^2 \quad (\text{A-10})$$

$$\mathcal{E}\{Q_k^2\} = \begin{cases} A^2(\frac{T^2}{2}\mathcal{E}_1\{1\} + 2\mathcal{E}_1\{\tau^2\}) + 2\sigma_n^2\mathcal{E}_1\{1\} & 0 \leq \tau < \frac{T}{2} \\ A^2(\frac{3T^2}{2}\mathcal{E}_2\{1\} - 4T\mathcal{E}_2\{\tau\} + 2\mathcal{E}_2\{\tau^2\}) + 2\sigma_n^2\mathcal{E}_2\{1\} & \frac{T}{2} \leq \tau < T \end{cases} \quad (\text{A-11})$$

$$\mathcal{E}\{I_k^4\} = A^4(T^4 - 4T^3\mathcal{E}\{\tau\} + 12T^2\mathcal{E}\{\tau^2\} - 16T\mathcal{E}\{\tau^3\} + 8\mathcal{E}\{\tau^4\}) + A^2\sigma_n^2(12T^2 - 24T\mathcal{E}\{\tau\} + 24\mathcal{E}\{\tau^2\}) + 12\sigma_n^4 \quad (\text{A-12})$$

$$\mathcal{E}\{Q_k^4\} = \begin{cases} A^4(\frac{T^4}{2}\mathcal{E}_1\{1\} + 8\mathcal{E}_1\{\tau^4\}) \\ \quad + A^2\sigma_n^2(6T^2\mathcal{E}_1\{1\} + 24\mathcal{E}_1\{\tau^2\}) + 12\sigma_n^4\mathcal{E}_1\{1\} & 0 \leq \tau < \frac{T}{2} \\ A^4(\frac{17T^4}{2}\mathcal{E}_2\{1\} - 32T^3\mathcal{E}_2\{\tau\} + 48T^2\mathcal{E}_2\{\tau^2\} - 32T\mathcal{E}_2\{\tau^3\} + 8\mathcal{E}_2\{\tau^4\}) \\ \quad + A^2\sigma_n^2(30T^2\mathcal{E}_2\{1\} - 48T\mathcal{E}_2\{\tau\} + 24\mathcal{E}_2\{\tau^2\}) + 12\sigma_n^4\mathcal{E}_2\{1\} & \frac{T}{2} \leq \tau < T \end{cases} \quad (\text{A-13})$$

$$\mathcal{E}\{I_k^2 Q_k^2\} = \begin{cases} A^4(\frac{T^4}{2}\mathcal{E}_1\{1\} + 2T^2\mathcal{E}_1\{\tau^2\} - 8T\mathcal{E}_1\{\tau^3\} + 8\mathcal{E}_1\{\tau^4\}) \\ \quad + A^2\sigma_n^2(5T^2\mathcal{E}_1\{1\} - 8T\mathcal{E}_1\{\tau\} + 16\mathcal{E}_1\{\tau^2\}) + 6\sigma_n^4\mathcal{E}_1\{1\} & 0 \leq \tau < \frac{T}{2} \\ A^4(\frac{3T^4}{2}\mathcal{E}_2\{1\} - 9T^3\mathcal{E}_2\{\tau\} + 15T^2\mathcal{E}_2\{\tau^2\} - 12T\mathcal{E}_2\{\tau^3\} + 4\mathcal{E}_2\{\tau^4\}) \\ \quad + A^2\sigma_n^2(7T^2\mathcal{E}_2\{1\} - 6T\mathcal{E}_2\{\tau\} + 4\mathcal{E}_2\{\tau^2\}) + 6\sigma_n^4\mathcal{E}_2\{1\} & \frac{T}{2} \leq \tau < T \end{cases} \quad (\text{A-14})$$

$$\mathcal{E}\{I_k^2 I_{k+1}^2\} = A^4(T^4 - 4T^3\mathcal{E}\{\tau\} + 8T^2\mathcal{E}\{\tau^2\} - 8T\mathcal{E}\{\tau^3\} + 4\mathcal{E}\{\tau^4\}) + A^2\sigma_n^2(4T^2 - 8T\mathcal{E}\{\tau\} + 8\mathcal{E}\{\tau^2\}) + 4\sigma_n^4 \quad (\text{A-15})$$

$$\mathcal{E}\{Q_k^2 Q_{k+1}^2\} = \begin{cases} A^4(\frac{T^4}{4}\mathcal{E}_1\{1\} + 2T^2\mathcal{E}_1\{\tau^2\} + 4\mathcal{E}_1\{\tau^4\}) \\ \quad + A^2\sigma_n^2(2T^2\mathcal{E}_1\{1\} + 8\mathcal{E}_1\{\tau^2\}) + 4\sigma_n^4\mathcal{E}_1\{1\} & 0 \leq \tau < \frac{T}{2} \\ A^4(\frac{25T^4}{4}\mathcal{E}_2\{1\} - 20T^3\mathcal{E}_2\{\tau\} + 26T^2\mathcal{E}_2\{\tau^2\} - 16T\mathcal{E}_2\{\tau^3\} + 4\mathcal{E}_2\{\tau^4\}) \\ \quad + A^2\sigma_n^2(10T^2\mathcal{E}_2\{1\} - 16T\mathcal{E}_2\{\tau\} + 8\mathcal{E}_2\{\tau^2\}) + 4\sigma_n^4\mathcal{E}_2\{1\} & \frac{T}{2} \leq \tau < T \end{cases} \quad (\text{A-16})$$

$$\mathcal{E}\{I_k^2 Q_{k+1}^2\} = \begin{cases} A^4 \left( \frac{T^4}{2} \mathcal{E}_1\{1\} - T^3 \mathcal{E}_1\{\tau\} + 3T^2 \mathcal{E}_1\{\tau^2\} - 4T \mathcal{E}_1\{\tau^3\} + 4\mathcal{E}_1\{\tau^4\} \right) \\ \quad + A^2 \sigma_n^2 (3T^2 \mathcal{E}_1\{1\} - 4T \mathcal{E}_1\{\tau\} + 8\mathcal{E}_1\{\tau^2\}) + 4\sigma_n^4 \mathcal{E}_1\{1\} & 0 \leq \tau < \frac{T}{2} \\ A^4 \left( \frac{6T^4}{2} \mathcal{E}_2\{1\} - 9T^3 \mathcal{E}_2\{\tau\} + 15T^2 \mathcal{E}_2\{\tau^2\} - 12T \mathcal{E}_2\{\tau^3\} + 4\mathcal{E}_2\{\tau^4\} \right) \\ \quad + A^2 \sigma_n^2 (7T^2 \mathcal{E}_2\{1\} - 12T \mathcal{E}_2\{\tau\} + 8\mathcal{E}_2\{\tau^2\}) + 4\sigma_n^4 \mathcal{E}_2\{1\} & \frac{T}{2} \leq \tau < T \end{cases} \quad (\text{A-17})$$

$$\mathcal{E}\{I_{k+1}^2 Q_k^2\} = \begin{cases} A^4 \left( \frac{T^4}{2} \mathcal{E}_1\{1\} - T^3 \mathcal{E}_1\{\tau\} + 3T^2 \mathcal{E}_1\{\tau^2\} - 4T \mathcal{E}_1\{\tau^3\} + 4\mathcal{E}_1\{\tau^4\} \right) \\ \quad + A^2 \sigma_n^2 (5T^2 \mathcal{E}_1\{1\} - 2T \mathcal{E}_1\{\tau\} + 4\mathcal{E}_1\{\tau^2\}) + 6\sigma_n^4 \mathcal{E}_1\{1\} & 0 \leq \tau < \frac{T}{2} \\ A^4 \left( \frac{5T^4}{2} \mathcal{E}_2\{1\} - \frac{39T^3}{4} \mathcal{E}_2\{\tau\} + \frac{71T^2}{4} \mathcal{E}_2\{\tau^2\} - 15T \mathcal{E}_2\{\tau^3\} + 5\mathcal{E}_2\{\tau^4\} \right) \\ \quad + A^2 \sigma_n^2 (13T^2 \mathcal{E}_2\{1\} - 24T \mathcal{E}_2\{\tau\} + 16\mathcal{E}_2\{\tau^2\}) + 6\sigma_n^4 \mathcal{E}_2\{1\} & \frac{T}{2} \leq \tau < T \end{cases} \quad (\text{A-18})$$

where, in the above equations

$$\mathcal{E}\{f(\tau)\} \triangleq \int_0^T f(\tau) p(\tau) d\tau \quad (\text{A-19})$$

$$\mathcal{E}_1\{f(\tau)\} \triangleq \int_0^{\frac{T}{2}} f(\tau) p(\tau) d\tau \quad (\text{A-20})$$

$$\mathcal{E}_2\{f(\tau)\} \triangleq \int_{\frac{T}{2}}^T f(\tau) p(\tau) d\tau \quad (\text{A-21})$$

where  $p(\tau)$  is the probability density function of the variable  $\tau$ .

## Appendix B

### Derivation of the Mean and Variance of the AVOD

Note that the calculations in this appendix incorporate the results of Appendix C. The inphase and quadrature outputs are given, respectively, by Eqs. (13) and (14). The lock detector output  $X_k = |I_k| - |Q_k|$ . Let  $\mu_k = \mathcal{E}\{|I_k| - |Q_k|\}$ . Then,

$$\begin{aligned} \text{Var}(X_k) &= \mathcal{E}\{|I_k| - |Q_k|\}^2 - \mu_k^2 \\ &= \mathcal{E}\{I_k^2 + Q_k^2 - 2|I_k Q_k|\} - \mu_k^2 \end{aligned} \quad (\text{B-1})$$

and

$$\begin{aligned} \text{Cov}(X_k, X_{k+j}) &= \mathcal{E}\{|I_k| - |Q_k| - \mu_k\}\{|I_{k+j}| - |Q_{k+j}| - \mu_{k+j}\} \\ &= \mathcal{E}\{|I_k I_{k+j}|\} + \mathcal{E}\{|Q_k Q_{k+j}|\} - \mathcal{E}\{|I_k Q_{k+j}|\} - \mathcal{E}\{|I_{k+j} Q_k|\} - \mu_k \mu_{k+j} \end{aligned} \quad (\text{B-2})$$

The following equations were used to compute the variance of  $X_k$  and the covariance of  $X_k$  with  $X_{k+1}$ :

$$\mathcal{E}\{X_k\} = \begin{cases} \frac{1}{2}[\mathcal{E}_1\{|AT - 2A\tau + N|\}] - \mathcal{E}_1\{|2A\tau + N|\}] & 0 \leq \tau < \frac{T}{2} \\ \frac{1}{2}[\mathcal{E}_2\{|AT - 2A\tau + N|\}] - \mathcal{E}_2\{|2AT - 2A\tau + N|\}] & \frac{T}{2} \leq \tau < T \end{cases} \quad (\text{B-3})$$

$$\mathcal{E}\{|I_k Q_k|\} = \begin{cases} \frac{1}{2}[\mathcal{E}_1\{|(AT + N_1(k) + N_2(k))(AT + N_2(k) + N_1(k+1))|\}] \\ \quad + \mathcal{E}_1\{|(AT - 2A\tau + N_1(k) + N_2(k))(-2A\tau + N_2(k) + N_1(k+1))|\}] & 0 \leq \tau < \frac{T}{2} \\ \frac{1}{4}[\mathcal{E}_2\{|(AT + N_1(k) + N_2(k))(AT + N_2(k) + N_1(k+1))|\}] \\ \quad + \mathcal{E}_2\{|(AT + N_1(k) + N_2(k))(2AT - 2A\tau + N_2(k) + N_1(k+1))|\}] \\ \quad + \mathcal{E}_2\{|(AT - 2A\tau + N_1(k) + N_2(k))(2AT - 2A\tau + N_2(k) + N_1(k+1))|\}] \\ \quad + \mathcal{E}_2\{|(AT - 2A\tau + N_1(k) + N_2(k))(AT + N_2(k) + N_1(k+1))|\}] & \frac{T}{2} \leq \tau < T \end{cases} \quad (\text{B-4})$$

$$\begin{aligned} \mathcal{E}\{|I_k I_{k+1}|\} &= \frac{1}{4}[\mathcal{E}^2\{|AT + N_1(k) + N_2(k)\}|] \\ &\quad + \mathcal{E}\{|(AT - 2A\tau + N_1(k) + N_2(k))(AT - 2A\tau + N_1(k+1) + N_2(k+1))|\}] \\ &\quad + 2\mathcal{E}\{|AT + N_1(k) + N_2(k)\}\mathcal{E}\{|AT - 2A\tau + N_1(k+1) + N_2(k+1)\}|] \end{aligned} \quad (\text{B-5})$$

$$\mathcal{E}\{|Q_k Q_{k+1}\} = \begin{cases} \frac{1}{4}[\mathcal{E}_1^2\{|AT + N_1 + N_2|\} + \mathcal{E}_1\{|[2A\tau + N_1(k+1) + N_2(k)] \\ \times [2A\tau + N_1(k+2) + N_2(k+1)]|\}] \\ + 2\mathcal{E}\{|AT + N_1 + N_2|\}\mathcal{E}_1\{|[2A\tau + N_1 + N_2]|\}] & 0 \leq \tau < \frac{T}{2} \\ \frac{1}{4}[\mathcal{E}_2^2\{|AT + N_1 + N_2|\} + \mathcal{E}_2\{|[2AT - 2A\tau + N_1(k+1) + N_2(k)] \\ \times [2AT - 2A\tau + N_1(k+2) + N_2(k+1)]|\}] \\ + 2\mathcal{E}\{|AT + N_1 + N_2|\}\mathcal{E}_2\{|[2AT - 2A\tau + N_1 + N_2]|\}] & \frac{T}{2} \leq \tau < T \end{cases} \quad (\text{B-6})$$

$$\mathcal{E}\{|I_k Q_{k+1}\} = \begin{cases} \frac{1}{4}[\mathcal{E}^2\{|AT + N_1 + N_2|\} + \mathcal{E}_1\{|[2A\tau + N_1(k+1) + N_2(k)] \\ \times [AT - 2A\tau + N_1(k+2) + N_2(k+1)]|\}] \\ + 2\mathcal{E}\{|AT + N_1 + N_2|\}\mathcal{E}_1\{|[2A\tau + N_1 + N_2]|\}] & 0 \leq \tau < \frac{T}{2} \\ \frac{1}{4}[\mathcal{E}^2\{|AT + N_1 + N_2|\} + \mathcal{E}_2\{|[AT - 2A\tau + N_1(k+1) + N_2(k)] \\ \times [2AT - 2A\tau + N_1(k+2) + N_2(k+1)]|\}] \\ + 2\mathcal{E}\{|AT + N_1 + N_2|\}\mathcal{E}\{|[AT - 2A\tau + N_1 + N_2]|\}] & \frac{T}{2} \leq \tau < T \end{cases} \quad (\text{B-7})$$

$$\mathcal{E}\{|I_{k+1} Q_k\} = \begin{cases} \frac{1}{4}[\mathcal{E}_1\{|[AT + N_1(k+1) + N_2(k+1)][AT + N_1(k+1) + N_2(k)]|\}] \\ + \mathcal{E}_1\{|[AT - 2A\tau + N_1(k+1) + N_2(k+1)][AT + N_1(k+1) + N_2(k)]|\}] \\ + \mathcal{E}_1\{|[AT - 2A\tau + N_1(k+1) + N_2(k+1)][2A\tau + N_1(k+1) + N_2(k)]|\}] \\ + \mathcal{E}_1\{|[AT + N_1(k+1) + N_2(k+1)][2A\tau + N_1(k+1) + N_2(k)]|\}] & 0 \leq \tau < \frac{T}{2} \\ \frac{1}{2}[\mathcal{E}_2\{|[AT - 2A\tau + N_1(k+1) + N_2(k+1)][2AT - 2A\tau + N_1(k+1) + N_2(k)]|\}] \\ + \mathcal{E}_2\{|[AT + N_1(k+1) + N_2(k+1)][AT + N_1(k+1) + N_2(k)]|\}] & \frac{T}{2} \leq \tau < T \end{cases} \quad (\text{B-8})$$

where  $\mathcal{E}_1$  and  $\mathcal{E}_2$  are defined in Appendix A. The following functions were defined to obtain the results in Subsection III.A of the main text.

$$F_1(\eta_s) \triangleq \mathcal{E}\{|(1 + cn_1 + cn_2)(1 + cn_2 + cn_3)|\}$$

$$F_2(\eta_s) \triangleq \mathcal{E}\{|(1 + cn_1 + cn_2)(cn_2 + cn_3)|\}$$

$$F_3(\eta_s) \triangleq \mathcal{E}\{|(1 - 2u + cn_1 + cn_2)(1 - 2u + cn_3 + cn_4)|\}$$

$$G_1(\eta_s) \triangleq \mathcal{E}_1\{|(1 - 2u + cn_1 + cn_2)(2u + cn_2 + cn_3)|\}$$

$$G_2(\eta_s) \triangleq \mathcal{E}_1\{|(1 - 2u + cn_1 + cn_2)(1 + cn_2 + cn_3)|\}$$

$$G_3(\eta_s) \triangleq \mathcal{E}_1 \{ |(2u + cn_1 + cn_2)(2u + cn_3 + cn_4)| \}$$

$$G_4(\eta_s) \triangleq \mathcal{E}_1 \{ |(2u + cn_1 + cn_2)(1 - 2u + cn_3 + cn_4)| \}$$

$$H_1(\eta_s) \triangleq \mathcal{E}_2 \{ |(1 + cn_1 + cn_2)(2 - 2u + cn_2 + cn_3)| \}$$

$$H_2(\eta_s) \triangleq \mathcal{E} \{ |(1 - 2u + cn_1 + cn_2)(2 - 2u + cn_2 + cn_3)| \}$$

$$H_3(\eta_s) \triangleq \mathcal{E} \{ |(1 - 2u + cn_1 + cn_2)(1 + cn_2 + cn_3)| \}$$

$$H_4(\eta_s) \triangleq \mathcal{E} \{ |(2 - 2u + cn_1 + cn_2)(2 - 2u + cn_3 + cn_4)| \}$$

$$H_5(\eta_s) \triangleq \mathcal{E} \{ |(1 - 2u + cn_1 + cn_2)(2 - 2u + cn_3 + cn_4)| \} \tag{B-9}$$

where  $c \triangleq 1/(2\sqrt{\eta_s})$ , the  $n_i$ 's are normal independent random variables with zero mean and unit variance, and  $u$  is a uniform random variable in the range  $[0, 1]$ . In Fig. B-1, one plots these functions versus  $\eta_s$ . These functions have been computed as follows: In the  $F$  functions, the expectation with respect to  $u$  is carried over the entire region  $[0, 1]$ , while in  $G$  and  $H$  functions, the expectation is carried over  $[0, 1/2]$  and  $[1/2, 1]$ , respectively.

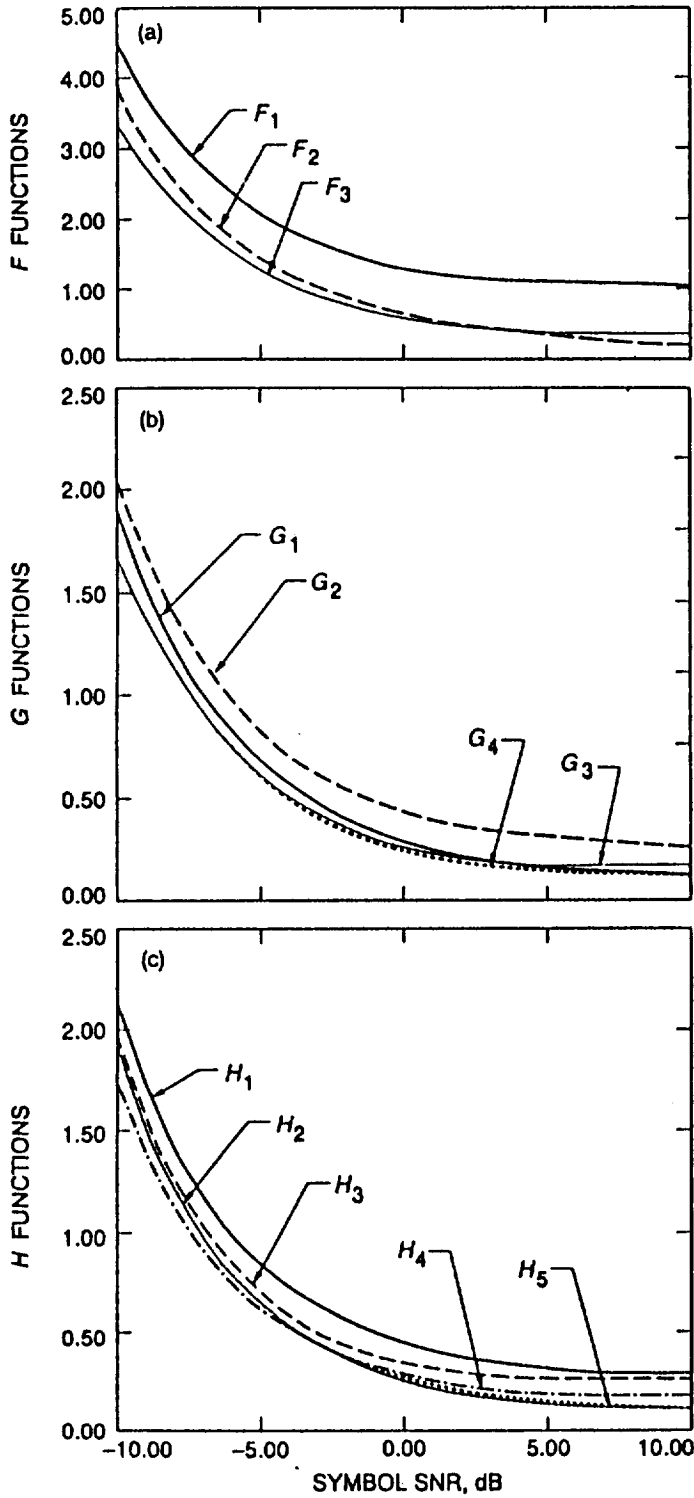


Fig. B-1. Function versus symbol SNR for: (a) *F* functions, (b) *G* functions, and (c) *H* functions.

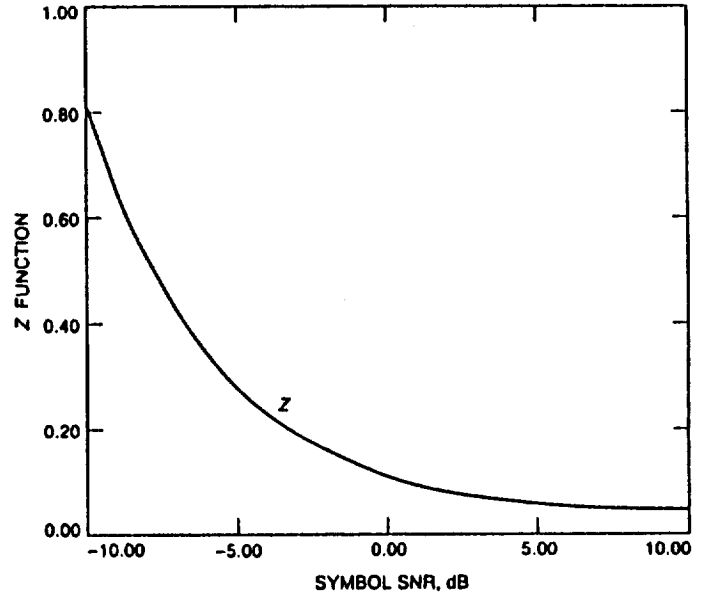


Fig. B-2. Z function versus symbol SNR.

## Appendix C

### Derivation of the Mean for the Random Variable $|n + b\tau + c|$

Let  $n$  be a normal random variable with zero mean and variance  $\sigma^2$ ,  $\tau$  a uniform random variable over  $(0, T)$ , and  $c$  any constant. Then,

$$\mathcal{E}\{|n + c|\} = \frac{1}{\sqrt{2\pi\sigma^2}} \int_{-\infty}^{\infty} |n + c| \exp\left(-\frac{n^2}{2\sigma^2}\right) dn \quad (\text{C-1})$$

The above integral can be easily evaluated by breaking it into two integrals over the two regions  $(-\infty, -c)$  and  $(-c, \infty)$  to obtain

$$\mathcal{E}\{|n + c|\} = \sqrt{\frac{2\sigma^2}{\pi}} \exp\left(-\frac{c^2}{2\sigma^2}\right) + c \operatorname{erf}\left(\frac{c}{\sqrt{2\sigma^2}}\right) \quad (\text{C-2})$$

For a fixed  $\tau$ , one can write

$$\mathcal{E}\{|n + b\tau + c|\} = \sqrt{\frac{2\sigma^2}{\pi}} \exp\left(-\frac{(b\tau + c)^2}{2\sigma^2}\right) + (b\tau + c) \operatorname{erf}\left(\frac{b\tau + c}{\sqrt{2\sigma^2}}\right) \quad (\text{C-3})$$

Unconditioning over  $\tau$  yields

$$\mathcal{E}_1\{|n + b\tau + c|\} = \frac{1}{T} \int_0^T \left[ \sqrt{\frac{2\sigma^2}{\pi}} \exp\left(-\frac{(b\tau + c)^2}{2\sigma^2}\right) + (b\tau + c) \operatorname{erf}\left(\frac{b\tau + c}{\sqrt{2\sigma^2}}\right) \right] d\tau \quad (\text{C-4})$$

which, after integration by parts, leads to

$$\begin{aligned} \mathcal{E}_1\{|n + b\tau + c|\} &= \frac{\sigma^2}{2bT} \left[ \operatorname{erf}\left(\frac{\frac{bT}{2} + c}{\sqrt{2\sigma^2}}\right) - \operatorname{erf}\left(\frac{c}{\sqrt{2\sigma^2}}\right) \right] + \frac{1}{2bT} \left[ \left(\frac{bT}{2} + c\right)^2 \operatorname{erf}\left(\frac{\frac{bT}{2} + c}{\sqrt{2\sigma^2}}\right) - c^2 \operatorname{erf}\left(\frac{c}{\sqrt{2\sigma^2}}\right) \right] \\ &+ \sqrt{\frac{\sigma^2}{2\pi}} \frac{1}{bT} \left[ \left(\frac{bT}{2} + c\right) \exp\left(-\frac{(\frac{bT}{2} + c)^2}{2\sigma^2}\right) - c \exp\left(-\frac{c^2}{2\sigma^2}\right) \right] \end{aligned} \quad (\text{C-5})$$

By applying the above expression, one gets

$$\mathcal{E}_1\{|AT - 2A\tau + N_1 + N_2|\} = \sqrt{N_0 T} \left[ \frac{1}{8\sqrt{\eta_s}} \operatorname{erf}(\sqrt{\eta_s}) + \frac{\sqrt{\eta_s}}{4} \operatorname{erf}(\sqrt{\eta_s}) + \frac{1}{4\sqrt{\pi}} \exp(-\eta_s) \right] \quad (\text{C-6})$$

Also, by simple manipulation, it can be shown that

$$\begin{aligned} \mathcal{E}_1\{|AT - 2A\tau + N_1 + N_2|\} &= \mathcal{E}_2\{|AT - 2A\tau + N_1 + N_2|\} \\ &= \mathcal{E}_1\{|2A\tau + N_1 + N_2|\} \\ &= \mathcal{E}_2\{|2AT - 2A\tau + N_1 + N_2|\} \end{aligned} \quad (\text{C-7})$$

## Appendix D

### Derivation of the Mean and Variance of the SQNOD

The samples  $I_k$  and  $Q_k$  are given by Eqs. (33) and (34). The moments of  $X_k$  are given by Eqs. (A-1) through (A-3). Using Eqs. (D-7) through (D-10) with  $\tau = 0$  and Eqs. (A-2) and (A-3) yields the in-lock variance. Namely,

$$\text{Var}(X_k) = \frac{A^4 T^4}{64} + \frac{3}{2} A^2 T^2 \sigma_n^2 + 4\sigma_n^4 \quad (\text{D-1})$$

The covariance can be shown to be, for  $j \geq 1$ ,

$$\text{Cov}(X_k, X_{k+j}) = 0 \quad (\text{D-2})$$

Similarly, with  $\tau$  modelled as uniform over  $[0, T/2]$  in Eqs. (D-7) through (D-10), the out-of-lock moments are found. Hence,

$$\text{Var}_o(X_k) = \frac{A^4 T^4}{60} + \frac{5}{3} A^2 T^2 \sigma_n^2 + 4\sigma_n^4 \quad (\text{D-3})$$

The out-of-lock covariance can be shown to be, for  $j \geq 1$ ,

$$\text{Cov}_o(X_k, X_{k+j}) = \frac{A^4 T^4}{120} \quad (\text{D-4})$$

The following equations are used in computing the variance of  $X_k$ :

$$\mathcal{E}\{I_k^2\} = \begin{cases} (\frac{A^2 T^2}{4} + \sigma_n^2) \mathcal{E}_1\{1\} & 0 \leq \tau < \frac{T}{4} \\ A^2 (\frac{5T^2}{8} \mathcal{E}_2\{1\} - 2T \mathcal{E}_2\{\tau\} + 2\mathcal{E}_2\{\tau^2\}) + \sigma_n^2 \mathcal{E}_2\{1\} & \frac{T}{4} \leq \tau < \frac{T}{2} \end{cases} \quad (\text{D-5})$$

$$\mathcal{E}\{Q_k^2\} = \begin{cases} A^2 (\frac{T^2}{8} \mathcal{E}_1\{1\} + 2\mathcal{E}_1\{\tau^2\}) + \sigma_n^2 \mathcal{E}_1\{1\} & 0 \leq \tau < \frac{T}{4} \\ (\frac{A^2 T^2}{4} + \sigma_n^2) \mathcal{E}_2\{1\} & \frac{T}{4} \leq \tau < \frac{T}{2} \end{cases} \quad (\text{D-6})$$

$$\mathcal{E}\{I_k^4\} = \begin{cases} (\frac{A^4 T^4}{16} + \frac{3}{2} A^2 T^2 \sigma_n^2 + 3\sigma_n^4) \mathcal{E}_1\{1\} & 0 \leq \tau < \frac{T}{4} \\ A^4 (\frac{17T^4}{32} \mathcal{E}_2\{1\} - 4T^3 \mathcal{E}_2\{\tau\} + 12T^2 \mathcal{E}_2\{\tau^2\} - 16T \mathcal{E}_2\{\tau^3\} + 8\mathcal{E}_2\{\tau^4\}) \\ \quad + A^2 \sigma_n^2 (\frac{15}{4} T^2 \mathcal{E}_2\{1\} - 12T \mathcal{E}_2\{\tau\} + 12\mathcal{E}_2\{\tau^2\}) + 3\sigma_n^4 \mathcal{E}_2\{1\} & \frac{T}{4} \leq \tau < \frac{T}{2} \end{cases} \quad (\text{D-7})$$

$$\mathcal{E}\{Q_k^4\} = \begin{cases} A^4 (\frac{T^4}{32} \mathcal{E}_1\{1\} + 8\mathcal{E}_1\{\tau^4\}) + A^2 \sigma_n^2 (\frac{3}{4} T^2 \mathcal{E}_1\{1\} + 12\mathcal{E}_1\{\tau^2\}) + 3\sigma_n^4 \mathcal{E}_1\{1\} & 0 \leq \tau < \frac{T}{4} \\ (\frac{A^4 T^4}{16} + \frac{3}{2} A^2 T^2 \sigma_n^2 + 3\sigma_n^4) \mathcal{E}_2\{1\} & \frac{T}{4} \leq \tau < \frac{T}{2} \end{cases} \quad (\text{D-8})$$

## Appendix E

### Derivation of the Mean and Variance of the AVNOD

By following the same procedure as in Appendix B and by using

$$\mathcal{E}\{|I_k|\} = \begin{cases} \mathcal{E}_1\left\{\left|\frac{AT}{2} + N\right|\right\} & 0 \leq \tau < \frac{T}{4} \\ \frac{1}{2}[\mathcal{E}_2\left\{\left|\frac{AT}{2} + N\right|\right\} + \mathcal{E}_2\{|AT - 2A\tau + N|\}] & \frac{T}{4} \leq \tau < \frac{T}{2} \end{cases} \quad (\text{E-1})$$

$$\mathcal{E}\{|Q_k|\} = \begin{cases} \frac{1}{2}[\mathcal{E}_1\left\{\left|\frac{AT}{2} + N\right|\right\} + \mathcal{E}_1\{|2A\tau + N|\}] & 0 \leq \tau < \frac{T}{4} \\ \mathcal{E}_2\left\{\left|\frac{AT}{2} + N\right|\right\} & \frac{T}{4} \leq \tau < \frac{T}{2} \end{cases} \quad (\text{E-2})$$

and

$$\text{Var}(|I_k| - |Q_k|) = \begin{cases} \begin{aligned} & \frac{3A^2T^2}{8}\mathcal{E}_1\{1\} + 2A^2\mathcal{E}_1\{\tau^2\} + 2\sigma_n^2\mathcal{E}_1\{1\} \\ & - \frac{5}{4}\mathcal{E}_1^2\left\{\left|\frac{AT}{2} + N\right|\right\} - \frac{1}{4}\mathcal{E}_1^2\{|2A\tau + N|\} \\ & - \frac{1}{2}\mathcal{E}\left\{\left|\frac{AT}{2} + N\right|\right\}\mathcal{E}_1\{|2A\tau + N|\} \end{aligned} & 0 \leq \tau < \frac{T}{4} \\ \begin{aligned} & \frac{7A^2T^2}{8}\mathcal{E}_2\{1\} - 2A^2T\mathcal{E}_2\{\tau\} + 2A^2\mathcal{E}_2\{\tau^2\} + 2\sigma_n^2\mathcal{E}_2\{1\} \\ & - \frac{5}{4}\mathcal{E}_2^2\left\{\left|\frac{AT}{2} + N\right|\right\} - \frac{1}{4}\mathcal{E}_2^2\{|AT - 2A\tau + N|\} \\ & - \frac{1}{2}\mathcal{E}\left\{\left|\frac{AT}{2} + N\right|\right\}\mathcal{E}_2\{|AT - 2A\tau + N|\} \end{aligned} & \frac{T}{4} \leq \tau < \frac{T}{2} \end{cases} \quad (\text{E-3})$$

one obtains Eqs. (40) through (45) after using the results of Appendix C and lengthy manipulations. The function  $Z$  in Eq. (45) is defined as

$$Z(\eta_s) \triangleq \mathcal{E}_1\{|(u + cn_1)(u + cn_2)|\} \quad (\text{E-4})$$

where  $c \triangleq 1/(2\sqrt{\eta_s})$ , the  $n_i$ 's are normal independent random variables with zero mean and unit variance, and  $u$  is a uniform random variable in the range  $(0, 1)$ . In  $Z$ , the expectation with respect to  $u$  is over the range  $[0, 1/4]$  and the function is plotted in Fig. B-2 versus the symbol SNR  $(\eta_s)$ .

## Appendix F

## Derivation of the Mean and Variance of the SPED

The samples  $I_k$  and  $Q_k$  are given by Eqs. (47) and (48). The output of the lock detector is  $x_k = I_k Q_k$ . It is straightforward to show that

$$\mathcal{E}\{X_k\} = \frac{A^2 T^2}{4} - \frac{A^2 T}{2} \mathcal{E}\{\tau\} \quad (\text{F-1})$$

and

$$\mathcal{E}\{X_k^2\} = A^4 \left( \frac{T^4}{16} - \frac{T^3 \mathcal{E}\{\tau\}}{4} + \frac{T^2 \mathcal{E}\{\tau^2\}}{2} \right) + \sigma_n^4 + A^2 \sigma_n^2 \left( \frac{T^2}{2} - T \mathcal{E}\{\tau\} + 2 \mathcal{E}\{\tau^2\} \right) \quad (\text{F-2})$$

$$\text{Cov}(X_k, X_{k+j}) = \begin{cases} \frac{A^4 T^2}{4} \text{Var}(\tau) & \tau \sim u(0, \frac{T}{2}) \text{ and } j \geq 1 \\ 0 & \tau = 0 \end{cases} \quad (\text{F-3})$$

Equations (49) and (50) follow after letting  $\tau = 0$  in Eqs. (F-1) through (F-3). Equations (51) and (52) follow by letting  $\tau$  be uniform over  $[0, T/2]$ .

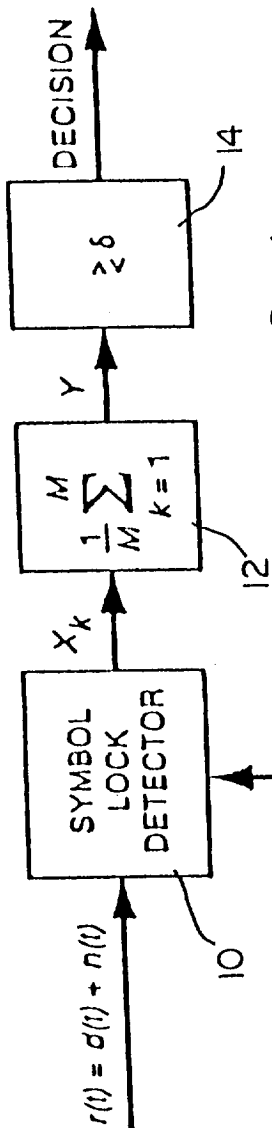


FIG. 1

SYMBOL TIMING  
(SYMBOL TIMING ERROR,  $\tau$ )

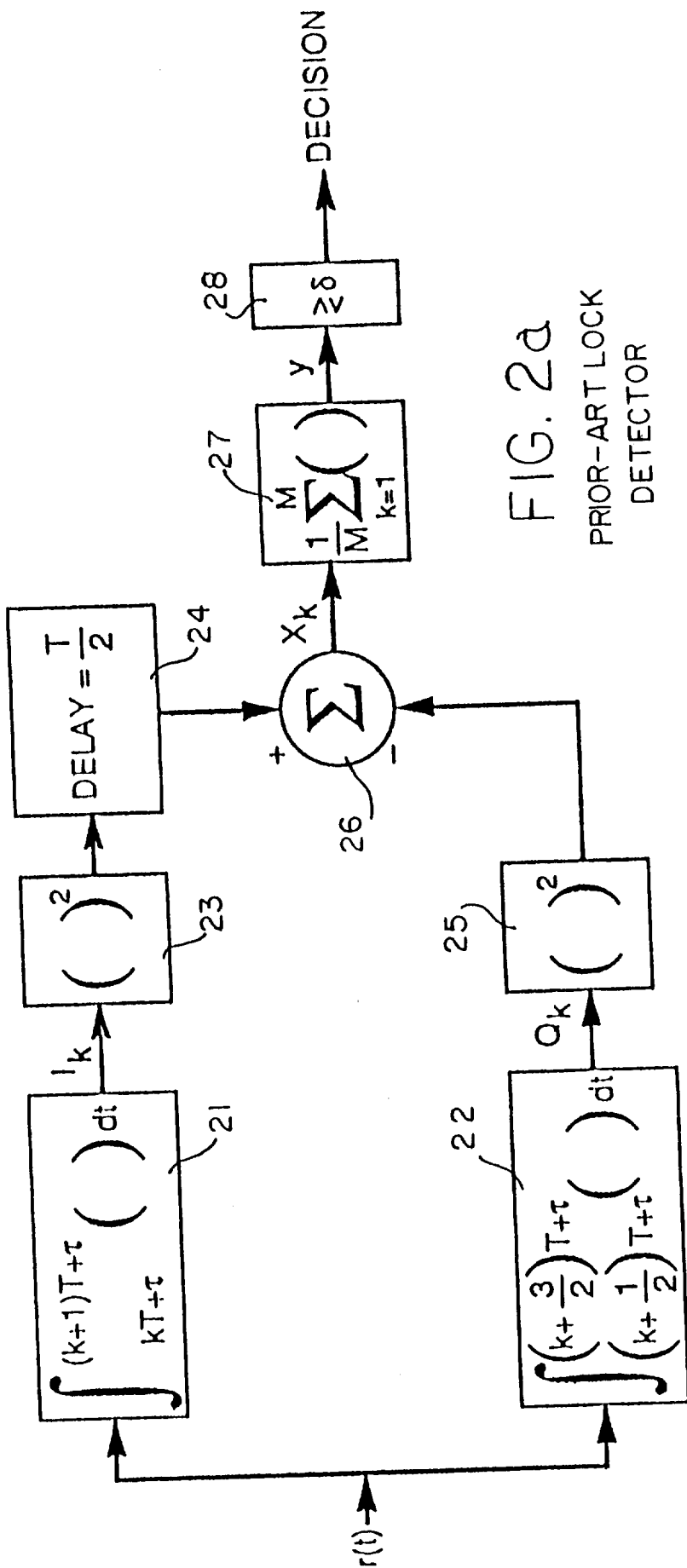


FIG. 2a  
PRIOR-ART LOCK  
DETECTOR

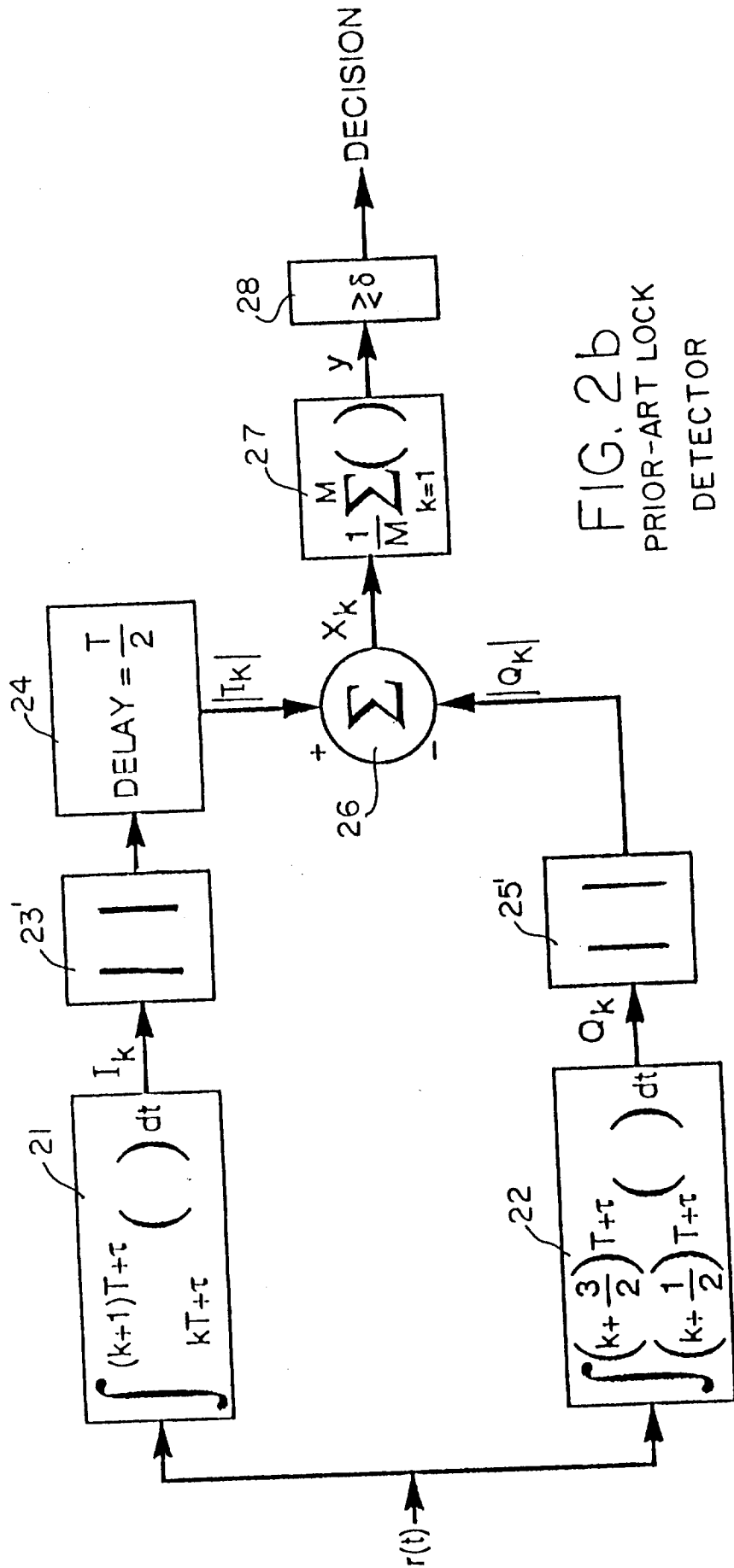


FIG. 2b  
PRIOR-ART LOCK  
DETECTOR

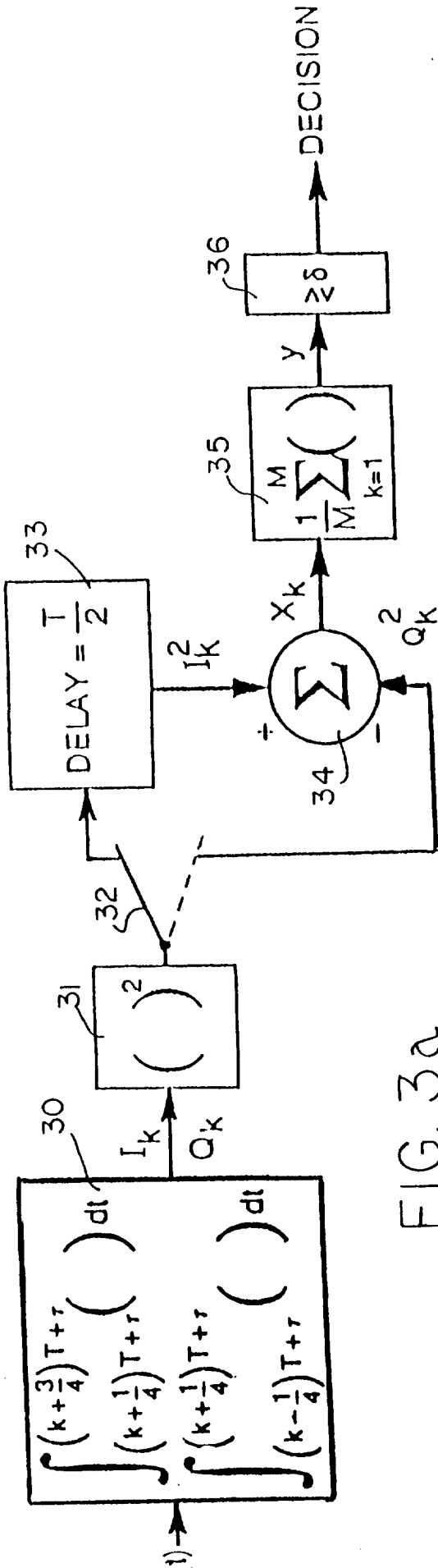


FIG. 3a

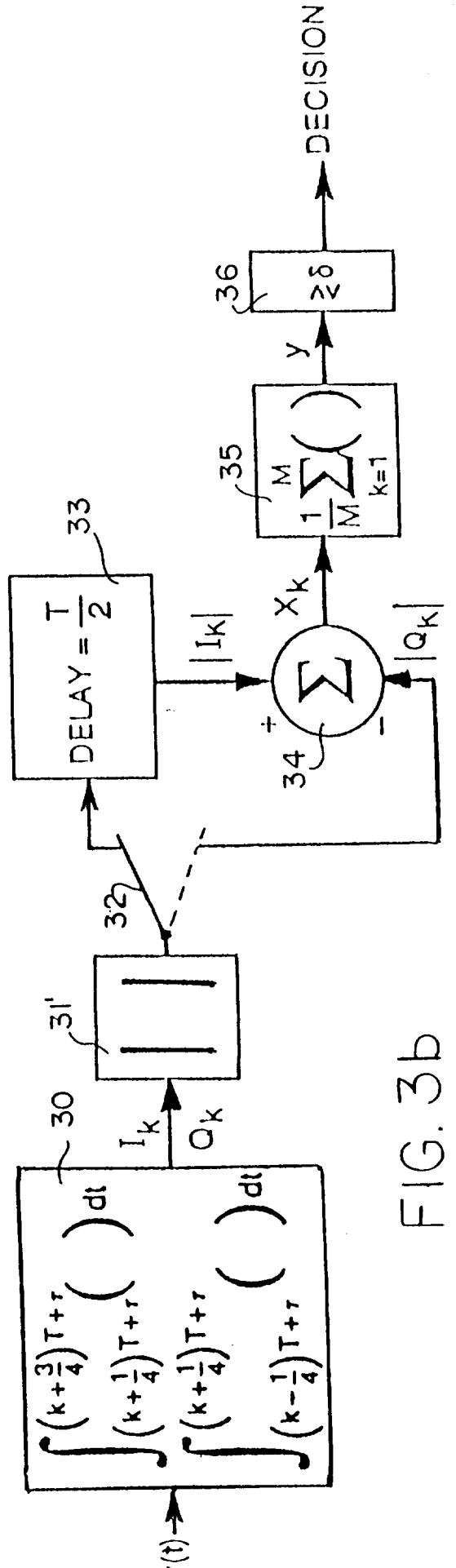


FIG. 3b

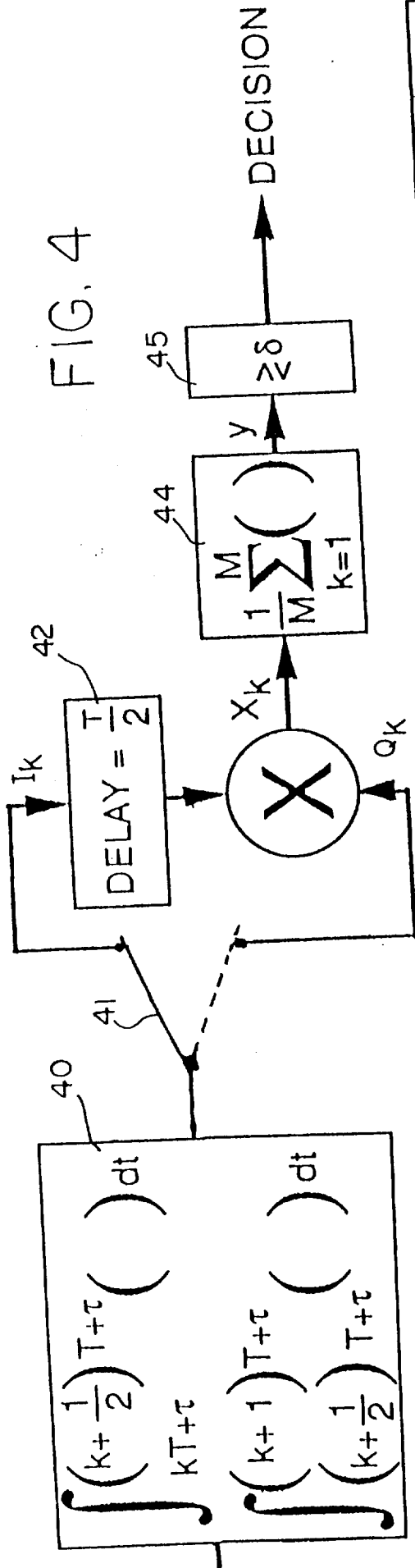


FIG. 4

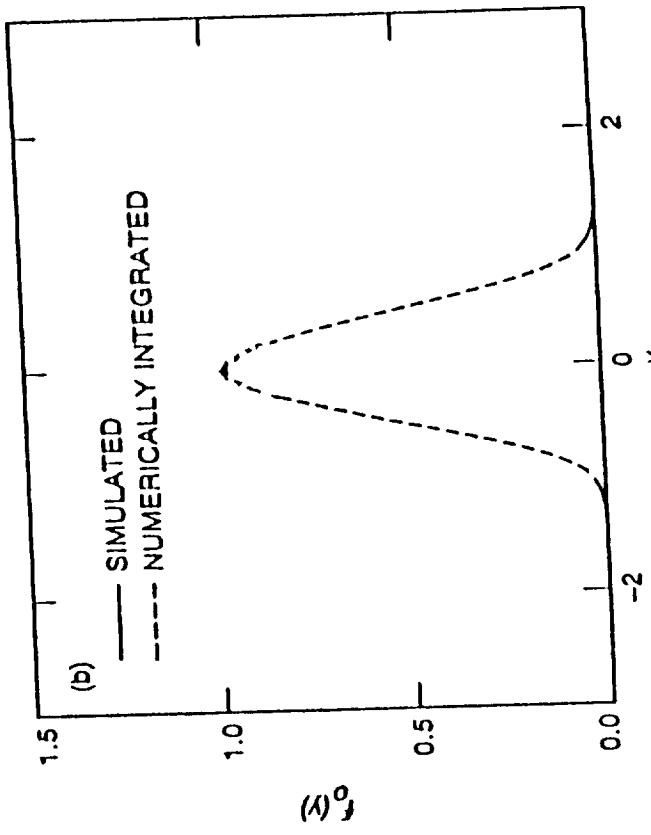


FIG. 5b

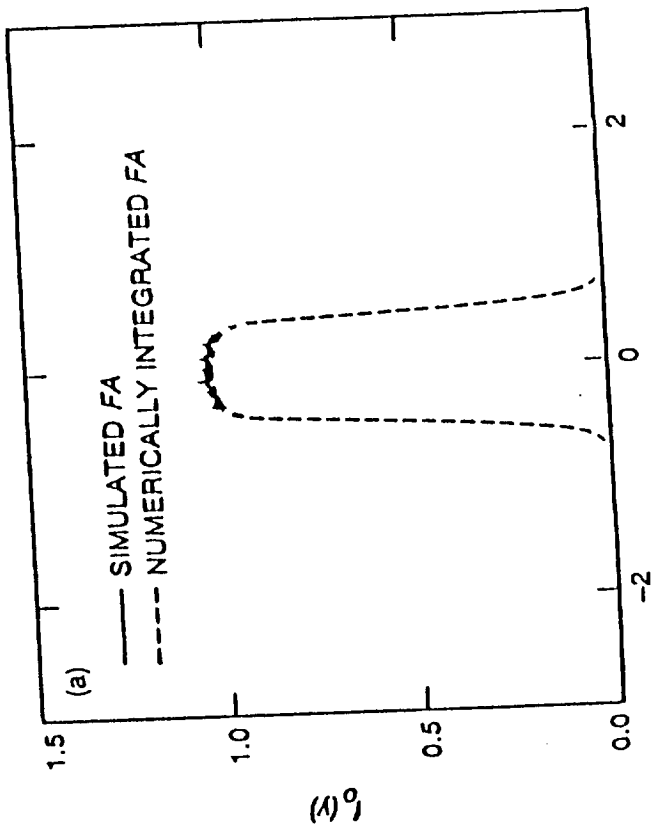


FIG. 5a

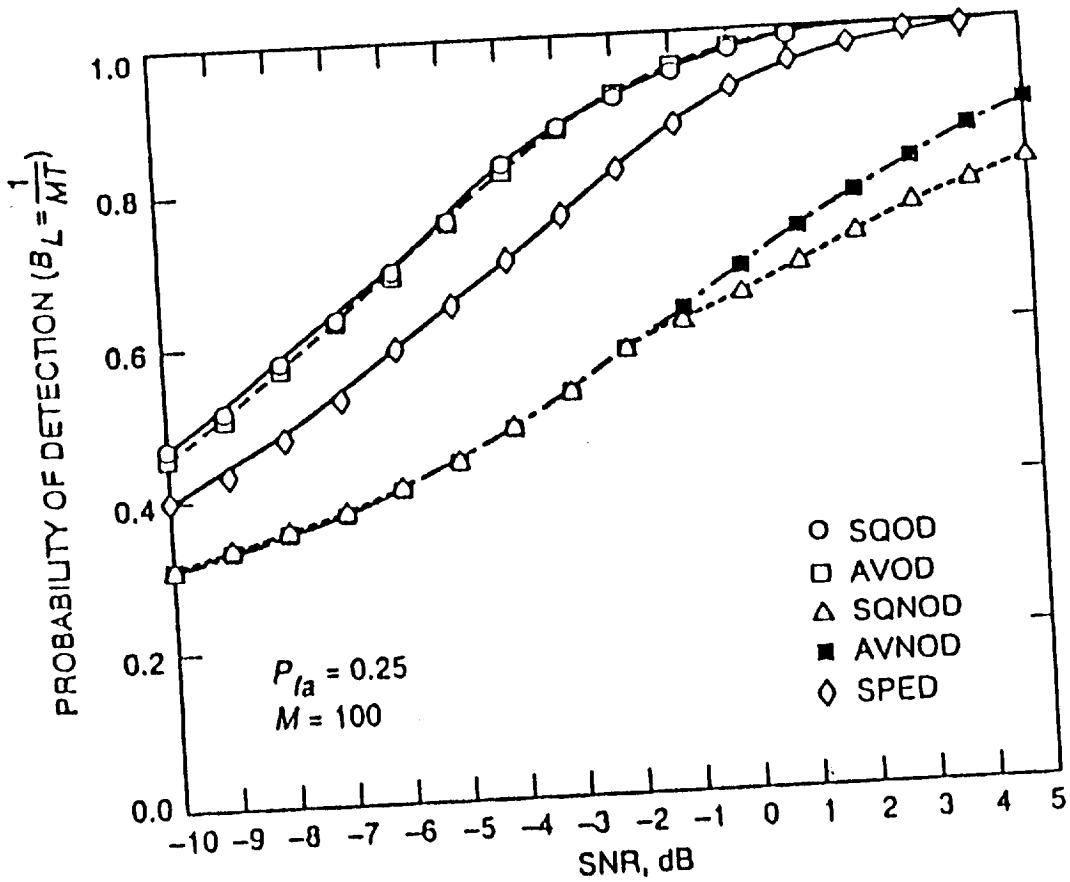


FIG. 6

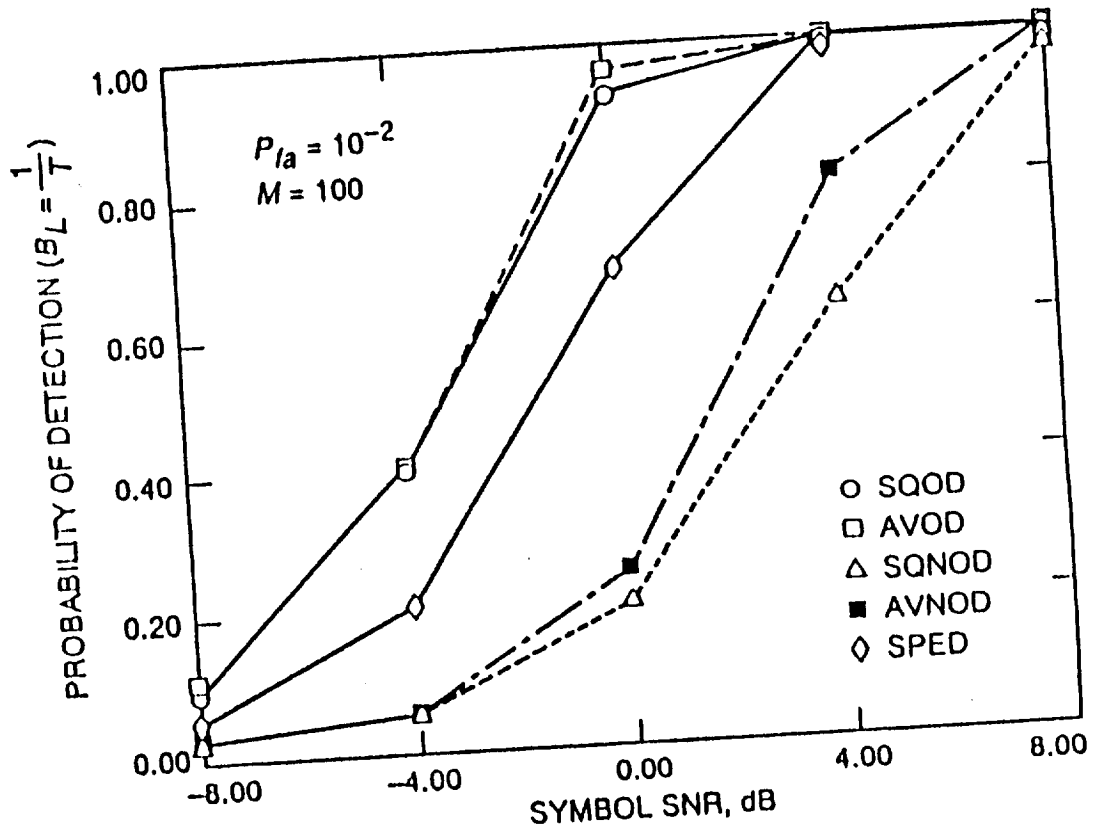


FIG. 7

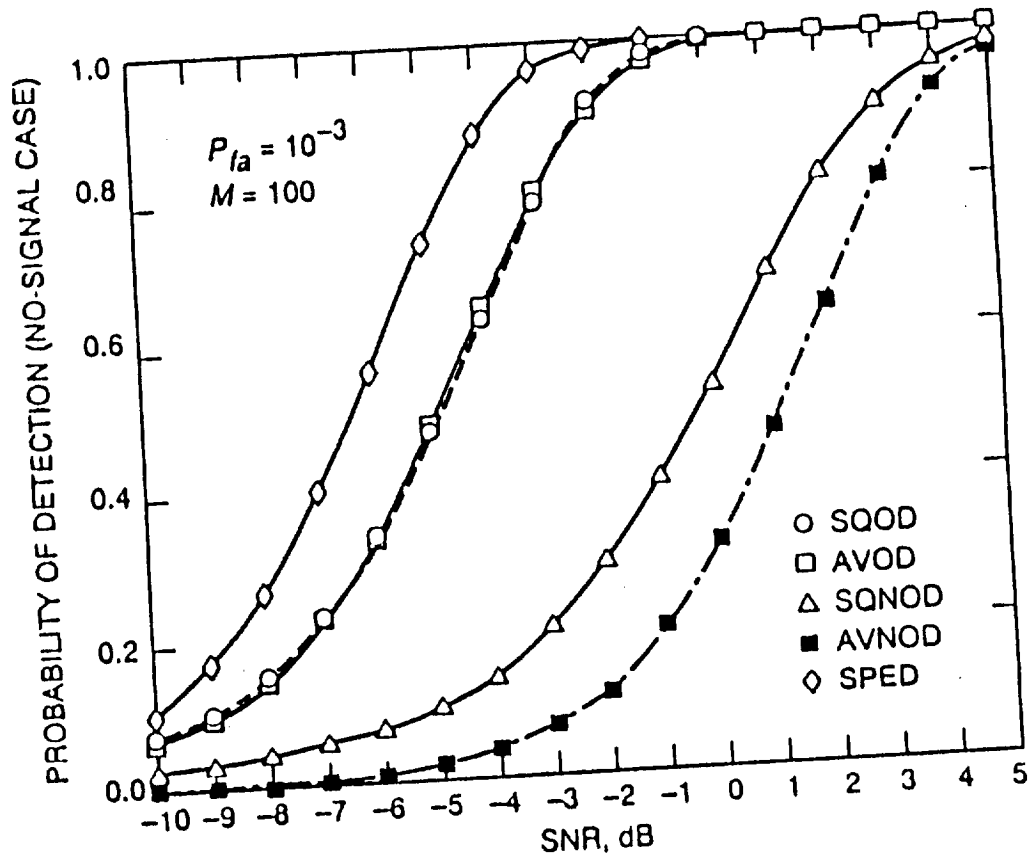


FIG. 8